HIF-transcribed p53 chaperones HIF-1α

Esha Madan[1], Taylor M. Parker[2,†], Christopher J. Pelham[3,†], Antonio M. Palma[1,†], Maria L. Peixoto[1], Masaki Nagane[4], Aliya Chandaria[5], Ana R. Tomás[1], Rita Canas-Marques[1], Vanessa Henriques[1], Antonio Galzerano[1], Joaquim Cabral-Teixeira[1], Karuppaiyah Selvendiran[6], Periannan Kuppusamy[7], Carlos Carvalho[1], Antonio Beltran[1], Eduardo Moreno[1], Uttam K. Pati[8] and Rajan Gogna ●[1,*]

[1]Champalimaud Centre for the Unknown, 1400-038 Lisbon, Portugal, [2]Department of Surgery, Simon Cancer Research Center, Indiana University School of Medicine, Indianapolis, IN 46202, USA, [3]Center for Clinical Pharmacology, Washington University School of Medicine and St. Louis College of Pharmacy, St. Louis, MO 63110, USA, [4]Department of Biochemistry, School of Veterinary Medicine, Azabu University, 1-17-71 Fuchinobe, Chuo-ku, Sagamihara, Kanagawa, 252-5201, Japan, [5]Biosciences unit, College of Life and Environmental Sciences, University of Exeter, Stocker Road Exeter EX4 4QD, UK, [6]Division of Gynecologic Oncology, Comprehensive Cancer Center, The Ohio State University Wexner Medical Center, Columbus, OH, USA, [7]Department of Radiology and Medicine, 601 Rubin Building, Norris Cotton Cancer Center, Geisel School of Medicine, Dartmouth College, 1 Medical Center Drive, Lebanon, NH 03756, USA and [8]Transcription and Human Biology Laboratory, School of Biotechnology, Jawaharlal Nehru University, New Delhi 110067, India

ABSTRACT

Chronic hypoxia is associated with a variety of physiological conditions such as rheumatoid arthritis, ischemia/reperfusion injury, stroke, diabetic vasculopathy, epilepsy and cancer. At the molecular level, hypoxia manifests its effects via activation of HIF-dependent transcription. On the other hand, an important transcription factor p53, which controls a myriad of biological functions, is rendered transcriptionally inactive under hypoxic conditions. p53 and HIF-1α are known to share a mysterious relationship and play an ambiguous role in the regulation of hypoxia-induced cellular changes. Here we demonstrate a novel pathway where HIF-1α transcriptionally upregulates both WT and MT p53 by binding to five response elements in p53 promoter. In hypoxic cells, this HIF-1α-induced p53 is transcriptionally inefficient but is abundantly available for protein-protein interactions. Further, both WT and MT p53 proteins bind and chaperone HIF-1α to stabilize its binding at its downstream DNA response elements. This p53-induced chaperoning of HIF-1α increases synthesis of HIF-regulated genes and thus the efficiency of hypoxia-induced molecular changes. This basic biology finding has important implications not only in the design of anti-cancer strategies but also for other physiological conditions where hypoxia results in disease manifestation.

INTRODUCTION

Hypoxia is a physiologically relevant biological stress that regulates organ development (1,2), homeostasis (3), wound healing (4,5), stroke (6,7) and cancer (2,8–19). Hypoxia induces transcriptional and molecular alterations which promote cell survival and growth under low oxygen conditions, by inducing gene expression programs controlling glucose uptake (20,21), metabolism (22–24), angiogenesis (25,26), erythropoiesis (27), cell proliferation (28), differentiation (29) and apoptosis (30).

Tumor hypoxia activates hypoxia-inducible factor (HIF). HIF molecular network is an important contributor towards cancer progression, and a variety of methods are adapted to block this pathway to achieve therapeutic utility (31–35). HIF proteins are transcription factors composed of an alpha subunit which is specifically stabilized in hypoxic conditions and a constitutively expressed β-subunit (ARNT) (36,37), which associates with the alpha subunit. Three HIF paralogs have been identified, HIF-1α, HIF-2α and HIF-3α (38–40), each with distinct functions in hypoxia. HIF-1α and HIF-2α display high structural similarity in their DNA binding domains, but differ in their trans-activation domains, indicating unique downstream gene

targets ([40–43](#)). HIF-1α has been shown to regulate genes involved in angiogenesis, most notably *VEGF* ([41](#)), as well as glycolysis ([42](#)), whereas HIF-2α has been shown to preferentially activate genes involved in stem cell maintenance and invasion ([40](#)). HIF-1α and HIF-2α also differ in their hypoxic induction pattern. HIF-1α protein levels are consistently detected rapidly within the first 2 h following hypoxia, whereas HIF-2α protein levels are detected later within 72 h post hypoxia exposure ([42,43](#)) HIF-3α differs in structure and acts as a negative regulator of HIF-1α and HIF-2α by competing with them for the availability of HIF β-subunits ([44,45](#)).

Another important transcription factor that regulates a myriad of cellular functions, including cell cycle, DNA repair, apoptosis, and metabolism, is tumor suppressor p53 ([46,47](#)). The *TP53* gene is mutated in nearly 50% of cancers, which frequently results in the full-length protein with increased stability, altered protein conformation and distinct biological activity from that of WT p53 protein ([48](#)). Regardless of the genetic status of p53, WT p53 is known to adopt a mutant-like conformation during the normal progression of the cell cycle ([49](#)) or by mitogenic stimulation ([50](#)), and most notably, within the hypoxic core of solid tumors ([11](#)). Given the altered conformation, MT, and MT-like p53 can be detected by a mutant conformation-specific polyclonal antibody, pAb240 ([51](#)). MT p53 is known to lose WT tumor-suppressive properties, but may also subvert WT p53 by exerting a dominant-negative effect on the remaining WT p53 via formation of inactivating co-aggregates ([52](#)). Additionally, MT gain of function (GOF) p53 is known to gain oncogenic functions and enhance tumor growth ([48,53](#)).

The role and activity of p53 under hypoxia are unclear ([8,54–56](#)), and the relationship between HIF-1α and p53 is ambiguous ([8,16,41,57–60](#)). p53 and HIF-1α are known to bind directly via the oxygen-dependent degradation domain of HIF-1α *in vitro*, as HIF-1α exists as an unfolded protein and becomes an easy target for protein-protein interaction with p53 ([61,62](#)). Such interactions with WT p53 are also found in MCF-7 cells carrying WT p53 ([13](#)) and in MT p53 cells ([60](#)). There are conflicting reports on the accumulation of p53 under hypoxic conditions and whether only MT, or WT or both forms of p53 protein show nuclear accumulation under hypoxia ([8,10,54,55,60](#)). We and others have found the accumulation of WT p53 under chronic hypoxia ([58,63](#)). Severe hypoxia or anoxia ($<0.2\%$ O_2) or the use of chemical agents result in the activation of p53, which can, in turn, lead to rapid apoptosis. In contrast, we along with others have reported that chronic hypoxia-induced p53 has little or no transcriptional capabilities and that hypoxic p53 loses key post-translational modifications which result in a transcriptionally inactive, conformational mutant phenotype for both WT and MT p53 molecules under physiologically relevant hypoxia of 1.8% O_2 ([11,54,63,64](#)). Thus, p53 was found to be both responsible and indispensable for apoptosis under hypoxia ([8,12,65–71](#)). It is likely that the use of random oxygen concentrations ranging from anoxia to 5% O_2, use of chemical stimulants for hypoxia and degree of reoxygenation, are possible reasons for these inconsistencies. There has been a lot of confusion about what definition of biological hypoxia ([21,72–75](#)) and under what conditions *in vitro* culture experiments should be performed to mimic physiologically relevant hypoxia ([76](#)). Many studies are performed using chemical stabilizers of HIF such as cobalt chloride ([60,77–79](#)) and deferoxamine ([80,81](#)), or under totally anoxic, i.e. 0% O_2 conditions ([82,83](#)) which are far from oxygen levels available in various diseases. Results from such variable conditions add to the misunderstandings and confusion in the field. Non-invasive electron paramagnetic resonance (EPR)-assisted measurement of oxygen in solid tumors shows that tumor oxygen concentration varies between 1.4% and 2% O_2 ([63,72,84](#)).

Because both HIF-1α and p53 are major transcription factors, and hypoxia is an essential and unavoidable physiological menace, it is necessary that a careful molecular study is performed under control settings using physiologically relevant hypoxia. This is the reason we have carefully based this study on measurement and simulation of physiological hypoxia using an EPR-based non-invasive technology in human xenografts and tumors in large animals such as rabbit.

In this study, we have used cancer as the physiological disease model to study HIF-1α-p53 relation. We present a newly discovered and biologically unavoidable role of both MT and WT p53 as tumor promoters in the hypoxic regions of solid tumors. HIF-1α, which is activated under hypoxia, induces p53 expression by directly binding to five response elements in *p53* promoter. HIF-1α-induced WT or MT p53 protein attains a transcriptionally inactive form under physiologically relevant hypoxia and forms a complex with HIF-1α. We found that both WT and MT p53 interact with HIF-1α and that HIF-1α-p53 complex remains functional while HIF-1α binds to the response elements (HREs) of its downstream target genes. In this complex p53 serves as a molecular chaperone for HIF-1α, it stabilizes HIF-1α and promotes its binding to the DNA response elements. This p53-assisted chaperoning of HIF-1α enhances HIF transcriptional activity thereby increasing the expression of HIF-regulated genes that contribute to hypoxia-induced growth and survival.

MATERIALS AND METHODS

Cell lines and culture conditions

p53 WT cancer cells including A375, IM-9, HepG2, SKCO-1, HeLa, MCF-7, U-87-MG, LNCaP-FGC, NCI-H711, HCT116, U2OS and *p53* MT cancer cells including MDA-MB-468, MOLT4, SW837, NCI-H23, P3HR1, PSN1, SKLMS1, SKLU1, SK-UT-1 and SNU-16 lines were procured from ATCC (VA, USA). HEK293T cells were procured from Cell BioLabs Inc. (San Diego, CA) and HEK293FT cells were procured by Thermo Fisher Scientific (MA, USA). Briefly, the cells were cultured in monolayer in respective growth mediums (Dulbecco's modified Eagle's medium (DMEM) or RPMI 1640) supplemented with 10% (v/v) heat-inactivated fetal bovine serum (FBS) and antibiotics (1% penicillin/streptomycin) and incubated under normoxic conditions at 37°C in a humidified atmosphere of 95% air and 5% CO_2.

Chemicals and constructs

Reagents including Lipofectamine® 3000 transfection reagent, Superscript Vilo cDNA synthesis kit, PowerUp SYBR Greenmaster mix, and DAB substrate kit were purchased from Thermo Fisher Scientific (MA, USA). MISSION Lentivirus Packaging Mix, human *p53* and *HIF-1α* shRNA (SHCLNG -NM_000546 and SHCLNG-NM_001530 respectively) lentiviral plasmid kit used for cell culture studies and hematoxylin and eosin stain were purchased from Sigma (CA, USA). *HIF-1α* lentiviral construct in EX-I0867-Lv105 vector was procured from Genecopoeia (MD, USA) and WT *p53* or MT (R175H) *p53* lentiviral expression vectors were used as described previously (85) and procured from Addgene (MA, USA). ViraSafe™ (Pantropic) Lentiviral Packaging System were purchased from Cell BioLabs (CA, USA). Antibodies used for IHC, anti-HIF1α (Rabbit monoclonal antibody to HIF-1α, AC-0108RUO), anti-p53 (Mouse monoclonal antibody to p53, P5813) and anti-Histone H3 (Rabbit polyclonal antibody to Histone H3, ab1791) were procured from Milipore-Sigma (CA, USA), Sigma-Aldrich (MO, USA) and Abcam (Cambrige, UK) respectively. Antibodies for western blot and immunoprecipitation anti-HIF1α (Mouse monoclonal antibody to HIF-1α, ab16066), anti-HIF1β (Mouse monoclonal antibody to HIF-1β, ab2771), anti-RNA polymerase II (Goat polyclonal antibody to RNA polymerase II, ab140509) and anti-α-Tubulin (Mouse monoclonal antibody to α-Tubulin, ab40742) were procured from Abcam, anti-p53 wild-type (Mouse monoclonal antibody to WT-p53, OP33) and anti-p53 mutant (Mouse monoclonal antibody to MT-p53, OP29L) were procured from Sigma-Aldrich, anti-p53 (Rabbit monoclonal antibody to p53, #2527) was procured from Cell Signaling Technology (MA, USA), anti-RNAse H II (Mouse monoclonal antibody to RNAse H II, sc-515475) and anti-β actin (mouse monoclonal antibody to β-actin, sc-517582) were procured from Santa-Cruz Biotechnology (TX, USA). Secondary antibodies anti-Mouse (Goat polyclonal secondary antibody to Mouse IgG - H&L (HRP), pre-adsorbed, ab97040), anti-Rabbit (Goat polyclonal secondary antibody to Rabbit IgG - H&L (HRP), pre-adsorbed, ab7090) and anti-goat (rabbit polyclonal secondary antibody to goat IgG - H&L (HRP), pre-adsorbed, ab97105) were procured from Abcam. PureLink RNA Mini Kit and RNeasy FFPE Kit were procured from Qiagen (CA, USA). Total protein extraction kit was purchased from Millipore (MA, USA). For luciferase reporter assay: five putative hypoxia-responsive elements (HREs) containing HIF-1α-binding consensus sequence 5′-R/CGTG -3′ (86) in the promoter region of *p53*; *VEGF*-HRE; *p21*-5′-DBS; *EPO*-HRE; *GAL4*; WT-*p53 GAL4*; MT-*p53 GAL4* and *p53* 10kb promoter were cloned in pGL4 luciferase vector purchased from Promega (WI, USA).

Gene silencing and overexpression

All work with lentiviruses was performed under BL2/BSL-2 conditions. Lentiviral production was performed using HEK293T cells. In brief, 2×10^4 cells per well in 96-well plate (supplemented with 10% fetal bovine serum and 4 mM L-glutamine, were allowed to grow overnight. HEK293T cells were transfected using Lipofectamine® 3000 per manufacturer instructions. Lentiviral supernatant was collected starting from 24–72 h post-transfection, filtered through a 0.45 μm filter and concentrated by ultracentrifugation. Titer of virus particles was determined using p24 ELISA (Cell BioLabs) as per the manufacturer's protocol, and a titer of 10^9 TU/ml was used for cell culture experiments. Target cells were infected with lentiviral supernatant containing 5 μg/ml of polybrene for 24 h. For the knockdown of both WT and MT *p53* (SHCLNG-NM_000546) and knockdown of *HIF-1α* shRNA (SHCLNG-NM_001530) lentiviral plasmid kit was procured from Sigma (CA, USA). For overexpression of *HIF-1α*, target cells were infected with lentiviral particles encoding with *HIF-1α* cDNA, EX-I0867-Lv105 vector, Genecopoeia (MD, USA).

Patient samples

For IHC staining, qPCR, ChIP and IPP studies, formaldehyde-fixed and paraffin-embedded and fresh frozen cancer tissue samples, including prostate, pancreatic, kidney, ovarian, colon, breast, lung and liver cancers, were procured from the Champalimaud Foundation, Lisbon, Portugal and Department of Pathology, UAMS, Little Rock, AR, USA.

Cycloheximide (CHX) chase assay

The half-life of HIF was measured using CHX chase assay. Approximately, 3×10^5 cells were seeded in 60 mm dishes and grown for 24 h. Then, the cells were cultured under hypoxia (1.8% O_2) for 24 h and treated with CHX (100 μg/ml) for 0, 3 and 6 h. The cells were collected at the indicated time points, and total protein lysates were prepared for western blotting to detect HIF-1α.

Immunohistochemistry

Champalimaud Foundation has a well-defined tissue banking protocol in which representative fresh samples from the tumor are stored immediately after gross sectioning, often < 1 h after the specimen is resected, in order to minimize protein degradation. Representative sections of the tumor were selected by expert pathologists, to analyze the expression of HIF-1α and p53 proteins immunohistochemically in paraffin-embedded tumor specimens fixed in 4% buffered formalin. Histological slides with 4 μm in thickness, were deparaffinized in xylol. Slides were heated in 0.01 M citrate buffer for 16 min in a microwave oven. After cooling for 20 min and washing in PBS, endogenous peroxidase was blocked with methanol containing 0.3% hydrogen peroxide for 30 min, followed by incubation with PBS containing 10% normal goat serum for 30 min. For immunohistochemical detection of HIF-1α, specimens were incubated overnight at 4°C with anti-HIF-1α at a dilution of 1:500. Visualization of bound antibodies was performed with streptavidin-biotin-peroxidase complex technique (Super Sensitive kit; BioGenex, CA, USA). As a chromogen, 3-amino-9-ethylcarbazole (BioGenex) was used. Expression of p53 was investigated with using a standard protocol (87).

In-vivo ELISA

The *in-vivo* ELISA was performed as described previously ([88]). Briefly, the wells of a PVC microtiter plate were coated with p53 WT or p53 MT antibodies at a concentration of 1–10 μg/ml in carbonate/bicarbonate buffer (pH 7.4). The plate was covered with an adhesive plastic and incubated overnight at 4°C. Next, the coating solution was removed, and the plate was washed twice with 200 μl PBS. Antibody-coated wells were blocked using 200 μl blocking buffer, 5% nonfat dry milk/PBS, and incubated overnight at 4°C. 5×10^4 cells were added to each well and incubated for 90 min at 37°C. 100 μl (0.5 μg/100 μl) of diluted detection antibody p53 WT or p53 MT was added to each well. The plate was covered with an adhesive plastic and incubated for 2 h at room temperature, then washed four times with PBS. 100 μl of secondary antibody conjugated with horseradish peroxidase (HRP) was added to the plate. The plate was covered with an adhesive plastic and incubated for 1–2 h at room temperature. The plate was washed four times with PBS, and O.D. was measured using ELISA reader.

RNA isolation and quantitative PCR (qPCR)

Total RNA from cell lines; and laser dissected patient cancer samples (hypoxic and normoxic zones) was isolated using the PureLink RNA Mini kit and RNeasy FFPE Kit, respectively. 10 ng of total RNA was reverse-transcribed to cDNA using Superscript Vilo cDNA synthesis kit. Real-time PCR (qPCR) was performed using a BioRad CFX96 and PowerUp SYBR Green master mix (Thermo Fisher Scientific). The following primers were used for the study: *p53* forward, 5′-ACCTATGGAAACTACTTCCTGAAA-3′ and reverse, 5′-CTGGCATTCTGGGAGCTTCA-3′; *HIF-1α* forward, 5′-CATAAAGTCTGCAACATGGAAGGT-3′ and reverse, 5′-ATTTGATGGGTGAGGAATGGGTT-3′; *GAPDH* forward, 5′-GGATGCAGGGAT GATGTTC-3′ and reverse, 5′-TGCACCACCAACTGCTTAG-3′. All reactions were set up in triplicates. Relative mRNA quantification was obtained using the comparative Ct method ($\Delta\Delta$Ct), and *GAPDH* served as an internal control, as described previously ([89]).

Hypoxia exposure

For hypoxic exposure, *p53* WT (A375. IM-9, HepG2, SKCO-1, HeLa, MCF-7, U-87-MG, LNCaP-FGC, NCI-H711, HCT116) and *p53* MT (MDA-MB-468, MOLT4, SW837, NCI-H23, P3HR1, PSN1, SKLMS1, SKLU1, SK-UT-1, SNU-16) cancer cells were placed into a humidified chamber maintained at 1.8% O_2 and 5% CO_2 (balance N_2) for 48 h, as described previously ([11,63,90]). As a control, cells were cultured in a standard incubator (normoxia; air with 5% CO_2).

In vitro transcription

In-vitro transcription reactions were carried out essentially as described previously ([85,91,92]), using 50 ng of G-less DNA templates. Nuclear extracts from the desired cell lines and template DNA were pre-incubated at room temperature for 10 min before nucleotides were added to the mixture. Reaction mixtures (20 μl) contained 2.5 mM NaF, 0.5 mM orthovanadate, 10 mM HEPES (pH 7.9), 12 mM Tris (pH 8.0), 0.1 mM EDTA, 12% glycerol, 60 mM KCl, 5 mM MgCl 2, 0.5 mM ATP, 0.5 mM UTP, 20 μM CTP, 0.25 mM O-methyl-GTP and 5 mM creatine phosphate. The DNA template contains six HIF-1α DNA binding sites at *VEGF* gene promoter upstream of the adenovirus major late (AdML) core promoter ([92]), a transcription initiation signal attached to a G-less cassette, a poly A signal, and finally a stop signal (CCT). The quantitative detection of the transcripts is done by conversion of the transcript to a cDNA form, using poly T primers, followed by qPCR using extension primers.

Immunoprecipitation (IP)

Immunoprecipitation experiments were performed as described previously ([93]). Briefly, nuclear extracts from cancer cells (WT, *p53* KO and *HIF-1α* KO) and tumor tissue samples (prostate, breast, kidney, lung, colon, liver, ovarian and pancreatic) were prepared using NE-PER Nuclear and Cytoplasmic Extraction Reagents (Thermo Fisher Scientific) using the provided protocol. Nuclear extracts were precleared for 1 h with Protein G PLUS-Agarose beads (Sigma). IP was then performed with 5μg of anti-p53 antibody or HIF-1α antibody on ice for 2 h. Then 10 μl of Protein G PLUS-agarose was added to the lysate and further incubated at 4°C for 4 h. Beads were washed three times in wash buffer (Nonidet P40 buffer: [20 mM Tris/HCl, pH 7.4, 100 mM NaCl, 10% (v/v) glycerol, 1.0% (v/v) Nonidet P40 and 1 mM EDTA]). Beads were then boiled at 95°C for 10 min in 2× SDS loading buffer.

Please refer to Supplementary file for detailed methods section.

RESULTS

HIF-1α correlates with WT and MT p53 expression in hypoxic cells and human tumors

p53 mRNA and protein expression are increased in hypoxic-cultured cells in relation to HIF-1α ([13,54,64,94]). We envisaged if these observations from *in vitro* setting hold true in physiologically relevant hypoxia observed in human tumors and whether expression of HIF-1α within intratumoral regions impacts p53 expression. Pancreatic (Figure 1A, top panel) and kidney (Figure 1A, bottom panel) cancer samples (FFPE) were H&E and immuno-stained for HIF-1α and p53 expression. Ten different areas, as demonstrated by rectangular boxes within each tumor, representing variability in HIF-1α expression, were selected (Figure 1A). These selected areas with variable HIF-1α expression are zoomed below each tumor. Signal intensity analysis points towards a positive dependent-relation between HIF-1α and p53 expression. Immunostaining for Histone H3 (a nuclear protein, like HIF-1α and p53) was performed as a control to quantify the variations in the expression of HIF-1α and p53 expression. No variations in Histone H3 staining (compared with HIF-1α and p53 expression) were observed in pancreatic and kidney cancer samples.
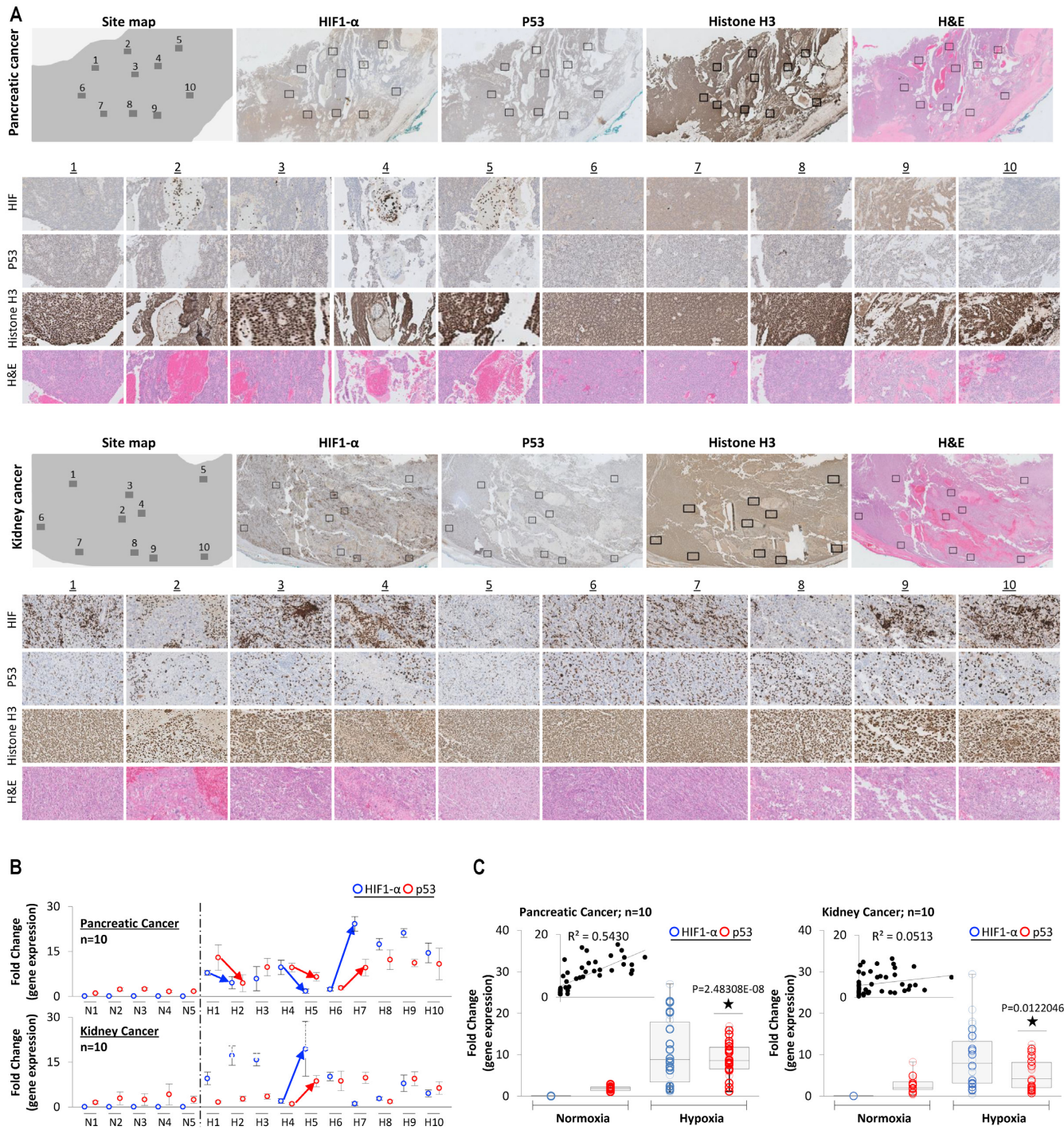
Figure 1. HIF-1α correlates with p53 expression in hypoxic zones of human cancers. (**A**) Immunohistochemical staining for p53 and HIF-1α shows their distribution in ten different regions of pancreatic and kidney tumors. The HIF-1α expression shows great intra-tumoral heterogeneity within the hypoxic microenvironment of both cancers. Ten fields marked 1–10 with variable HIF-1α expression were selected, and p53 expression in such areas was observed. A zoomed view (40×) of each of these ten fields shows high-resolution staining for HIF-1α and p53, H&E staining is used to locate the general structure of the tumor tissue. IHC with Histone H3 is used as control. (**B**) qPCR analysis was used to observe *p53* and *HIF-1α* gene expression in the ten selected regions, as shown in figure A. These 10 hypoxic regions were laser-captured, and gene expression was analyzed in triplicate. Normoxic regions were defined by negative HIF-1α staining; 5 such sites were selected, and gene expression was analyzed in triplicate. Blue and red arrows point towards easily observable trends for a simultaneous increase and decrease in *HIF-1α* and *p53* expression, respectively. (**C**) Box plots present collective data from 10 different areas and analyzed in triplicates in figure B and show increased expression of both *p53* (red) and *HIF-1α* (blue) in ten heterogeneous areas from single pancreatic and kidney cancer. Correlation coefficient analysis reveals $R^2 = 0.6247$ and $R^2 = 0.0882$ for pancreatic and kidney cancer, respectively ($n = 10$ for hypoxic regions, $n = 5$ for normoxic regions; all samples were analyzed in triplicates). Two-sided Student's *t*-test was used for analysis; all *P* values are labeled on the figure.

To quantify this relationship, these ten areas from pancreatic and kidney tumors were laser-captured and analyzed for the expression of *HIF-1α* and *p53* by qPCR (Figure 1B and C). Each laser-captured tissue section was analyzed in triplicates. For each tumor, five areas were selected and laser-captured to represent normoxia, which was defined by the absence of *HIF-1α* signal. In Figure 1B, expressions of *HIF-1α* and *p53* are represented within each rectangular area selection from Figure 1A. This provides an opportunity to see quantitative mRNA expression as well as protein expression (Supplementary Figure S1), for each selected area in both tumors. The correlation between the expression of HIF-1α and p53 is a bit weak at the protein level, possibly due to control of protein degradation rate, which is strongly relevant to HIF-1α. Normoxic regions showed lack of *HIF-1α* expression, but robust *p53* expression. In the hypoxic areas of both kidney and pancreatic tumors, *HIF-1α* was upregulated, although, the extent of upregulation varied between the examined sites. Additionally, *p53* expression significantly increased overall in hypoxic regions in both kidney and pancreatic tumors. Interestingly, *HIF-1α* and *p53* showed similar trends in expression in the ten examined sites. The arrows in Figure 1B, point towards such correlation; sites with strong and diffuse *HIF-1α* signal coincide with robust *p53* expression whereas sites with moderate or low *HIF-1* α show lower *p53* signal. Next, we determined the correlation between *HIF-1α* and *p53* expression under hypoxic and normoxic conditions (Figure 1C). In hypoxic regions, the data showed a strong positive correlation between the expression of *HIF-1α* and *p53* in a highly controlled setting as samples represent heterogeneous regions of the same tumor of pancreatic origin (R^2 and P values are labeled on the figure). In kidney cancer sample, although *p53* was upregulated in hypoxic regions, a strong correlation between *p53* and *HIF-1α* expression was not observed ($R^2 = 0.0513$).

We further expanded our *p53-HIF-1α* correlation analysis in a variety of human tumors including that of pancreas, kidney, colon, breast, lung, and liver (three patients for each tumor, analyzed in triplicates) (Figure 2A). Similar trends across all cancer types were identified, with the exception of lung cancer where the correlation between expression of *HIF-1α* and *p53* was weak ($R^2 = 0.1082$). Expression of *HIF-1α* is poor, but *p53* is robust in normoxic regions of the tumor. However, in the hypoxic regions, both *HIF-1α* and *p53* expressions are significantly higher. A strong correlation between *HIF-1α* and *p53* expression is observed in this large sample study from multiple cancers. Since *p53* is mutated in more than 50% tumors (95–97), we determined if the mutational status of *p53* has any impact on this observed correlation between *HIF-1α* and *p53* expression in hypoxic cell culture.

To arrive at a physiologically relevant hypoxia condition which should be used to culture the cell lines, we have used data from an ongoing clinical trial managed by our group and collaborators; please refer to the trial listing (https://clinicaltrials.gov/ct2/show/NCT02706197). Oxygen measurement data using state of the art non-invasive EPR spectroscopy (11) in 24 patients of breast cancer, squamous cell carcinoma and pancreatic ductal adenocarcinoma (unpublished data from the clinical trial), combined with our data in past using non-invasive electron paramagnetic resonance (EPR)-assisted measurement of oxygen in solid tumors shows that tumor oxygen concentration varies between 1.4% and 2% O_2 (63,72,84). Oxygen measurements by other groups in clinical cancer samples have also reported that oxygen concentration is around 1.7, 1.5, 1.2, 1.3, 2.2 and 1.8% O2 for brain, breast, cervical, renal, non-small-cell lung cancer and rectal cancer, respectively (72). Based on these findings, all hypoxia culture was established at this oxygen value (1.8% O_2). Ten *p53* wild-type (WT) and mutant (MT) cancer cell lines were cultured under hypoxic conditions. The *in vitro* results were similar to our observations in human clinical cancers; hypoxia led to an increase of both *p53* and *HIF-1α* expressions (Figure 2B and C) exhibiting a strong correlation between their expressions (Figure 2B).

HIF-1α regulates p53 expression in hypoxic cancer cells

Results from human tumors and cultured cells suggested a strong relationship between HIF-1α and p53 expressions. We next determined whether genetic manipulation of *HIF-1α* can achieve alterations in *p53* expression (Figure 3A and B). Five *p53* WT and five *p53* MT cancer cell lines were cultured under normoxic and hypoxic conditions. Empty backbone vectors and scrambled shRNAs were used as transfection controls and had no significant impact on gene expression (box plots 5, 6, 9, 10). Hypoxia-induced expression of both *HIF-1α* and *p53* when compared with normoxic conditions (compare box plots 1 & 2 with 3 & 4). *HIF-1α* shRNA reduced *HIF-1α* expression, but it also resulted in a significant reduction of *p53* expression in both WT and MT cells (box plots 7 & 8). The efficiency of *HIF-1α* and *p53* knockdown by shRNA is shown by Western blot (Figure 3A, inset). Exogenous addition of *HIF-1α* resulted in a significant increase in *p53* mRNA expression (box plots 11 & 12). These results suggest that HIF-1α can regulate p53 expression. To more thoroughly investigate HIF-1α genetic regulation of *p53*, we generated Crispr-assisted *HIF-1α* knockout (KO) MCF-7 cells (which carry a WT *p53*) and *HIF-1α* KO PSN1 cells (which carry MT *p53*) (Figure 3C). In *HIF-KO* (or *HIF-1α⁻/⁻*), hypoxia failed to stimulate *p53* expression; however, incremental treatment with *HIF-1α* cDNA in hypoxic-cultured MCF-7 and PSN1 cells rescued *p53* gene expression in a *HIF-1α* dose-dependent manner (lanes 3–6). In a western blot experiment, effect of HIF-1α on p53 protein expression was observed (Figure 3D). Normoxic MCF-7 and PSN1 cells show no HIF-1α expression and low p53 expression in both *HIF-1α* WT and KO lines (lanes 1 & 2). Hypoxia increases the expression of HIF-1α in the WT line, but KO line shows no expression of HIF-1α (lane 3 & 4). However, with the hypoxia-induced increase in HIF-1α expression p53 expression also increases but only in the WT line, in the *HIF-1α* KO line no such effect is observed both in WT (MCF-7) or MT (PSN1) p53 (Figure 3D). In another western blotting experiment, the effect of a dose-dependent increase in *HIF-1α* was observed on the expression of p53 in both normoxic and hypoxic *HIF-1α* WT MCF-7 and *HIF-1α* KO MCF-7 cells (Figure 3E). Under the normoxic condition, HIF-1α expression is not observed in both WT and KO MCF-7 cells and dose-dependent exogenous addition of *HIF-1α* also does not result in the expression of HIF-1α
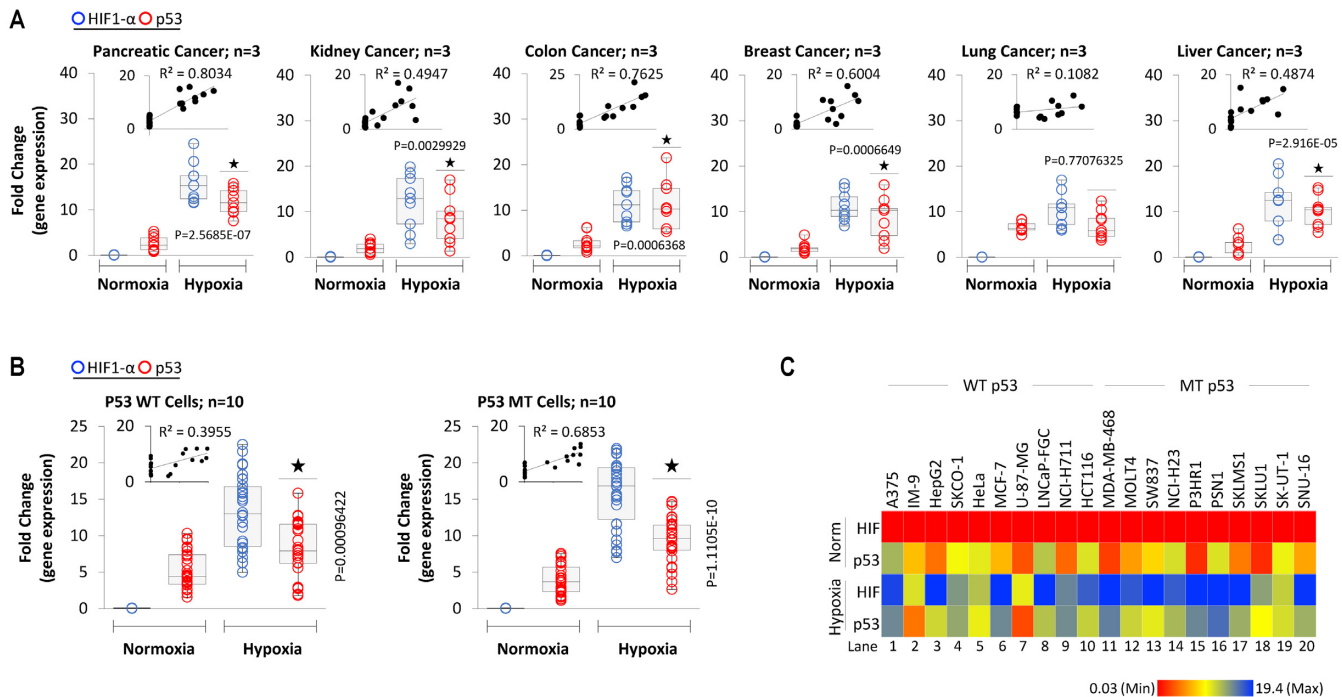
Figure 2. HIF-1α correlates with both WT and MT p53 in hypoxic cells and hypoxic cancer tissues. (**A**) Box plots represent qRT-PCR-based quantification of *p53* and *HIF-1α* gene expression in laser-captured hypoxic and normoxic regions of 6 different cancer types. For each cancer type, three different patient samples were collected, and from each sample, three different normoxic or hypoxic region were selected, thus for each cancer, three collected samples were analyzed in triplicates. The correlation coefficient between *HIF-1α* and *p53* mRNA expression was calculated for each cancer, and R^2 values are presented in the plots. Two-sided Student's *t*-test was used for analysis; all *P* values are labeled on the figure. (**B**) *p53* and *HIF-1α* gene expressions were quantified by qRT-PCR analysis from a panel of 10 WT *p53* and 10 MT *p53* cell lines (listed in 2C) cultured under normoxia or exposed to hypoxia (1.8% O_2) for 24 h. For each cell line, gene expression was analyzed on three independent replicates per *p53* WT or *p53* MT cell lines. Correlation coefficient analysis shows a positive correlation between *HIF-1α* and *p53* expression in MT *p53* and WT *p53* cell lines. Two-sided Student's *t*-test was used for analysis; all *P* values are labeled on the figure. (**C**) Heat map depicts *p53* and *HIF-1α* gene expression under normoxia and hypoxia for each WT *p53* and MT *p53* cancer cell line (quantified in 2C). *HIF-1α* and *p53* expression increased in all cell lines under hypoxia, irrespective of *p53* status. In this figure, each block represents the values from a gradient scale of low (red), medium (yellow) and high (blue) level of expression.

(lane 1–5). p53 expression in these cells also does not show any significant variation, and dose-dependent increase in *HIF-1α* does not increase p53 expression under normoxic conditions (lanes 1–5). *HIF-1α* WT MCF-7 cells show up-regulation of HIF-1α under hypoxic conditions, which also results in a significant increase in p53 expression (lane 6), this increase in p53 expression is reversed in *HIF-1α* KO MCF-7 cells cultured under hypoxic conditions, along with no expression of HIF-1α in the *HIF-1α* KO line (lane 7). Dose-dependent exogenous addition of *HIF-1α* in *HIF-1α* KO MCF-7 cells results in upregulation of both HIF-1α and p53 in a dose-dependent manner (lanes 8–10). This data shows that HIF-1α regulates p53 expression in hypoxic cancer cells.

HIF-1α transcriptionally regulates p53

Collectively, these findings suggest that hypoxia-stimulated HIF-1α regulates p53 expression at the transcriptional level. To further dissect this effect, we analyzed the activity of the full-length *p53* promoter (10kb; cloned in pGL4 luciferase vector) under the influence of HIF-1α (Figure 4A). Beta-galactosidase and empty pGL4 backbone vectors were used throughout the study in every luciferase assay as normalization controls. Since we are observing the impact of HIF-

1α in transcriptional regulation of the *p53* promoter, we included *VEGF* HIF response element (HRE) luciferase vector as a positive control of HIF-1α activity given that *VEGF* is a well-characterized target gene of HIF-1α under hypoxia (98). As expected, in WT *p53* MCF-7 cells under normoxia, *VEGF* HRE vector showed poor activity, which is expected because of poor HIF-1α expression (bar 3). The *p53* 10kb promoter was active in normoxia, and *HIF-1α* shRNA did not impact this activity (bars 5 & 6). p53 downstream gene, *p21*, has a p53 DNA binding site (DBS) and its activity in the presence of doxorubicin (p53 transcriptional activator) was observed as a positive control in normoxia (93) (bar 7). In hypoxic culture conditions, HRE-containing *VEGF* promoter showed a significant increase in activity (positive control; bar 10), which is expected as HIF-1α expression is observed in hypoxia. This effect was reversed upon addition of *HIF-1α* shRNA (negative control; bar 11). Interestingly, the activity of full *p53* promoter was significantly increased under hypoxic conditions but was reversed upon addition of *HIF-1α* shRNA (bars 12 & 13), suggesting transcriptional regulation of *p53* by HIF-1α. The data comparing *p53* promoter activity in *HIF-1α* shRNA treated normoxic and hypoxic cells (bars 6 & 13), indicates that under normoxia *p53* promoter is regulated independent of HIF-1α, but in hypoxic conditions, this transcription factor
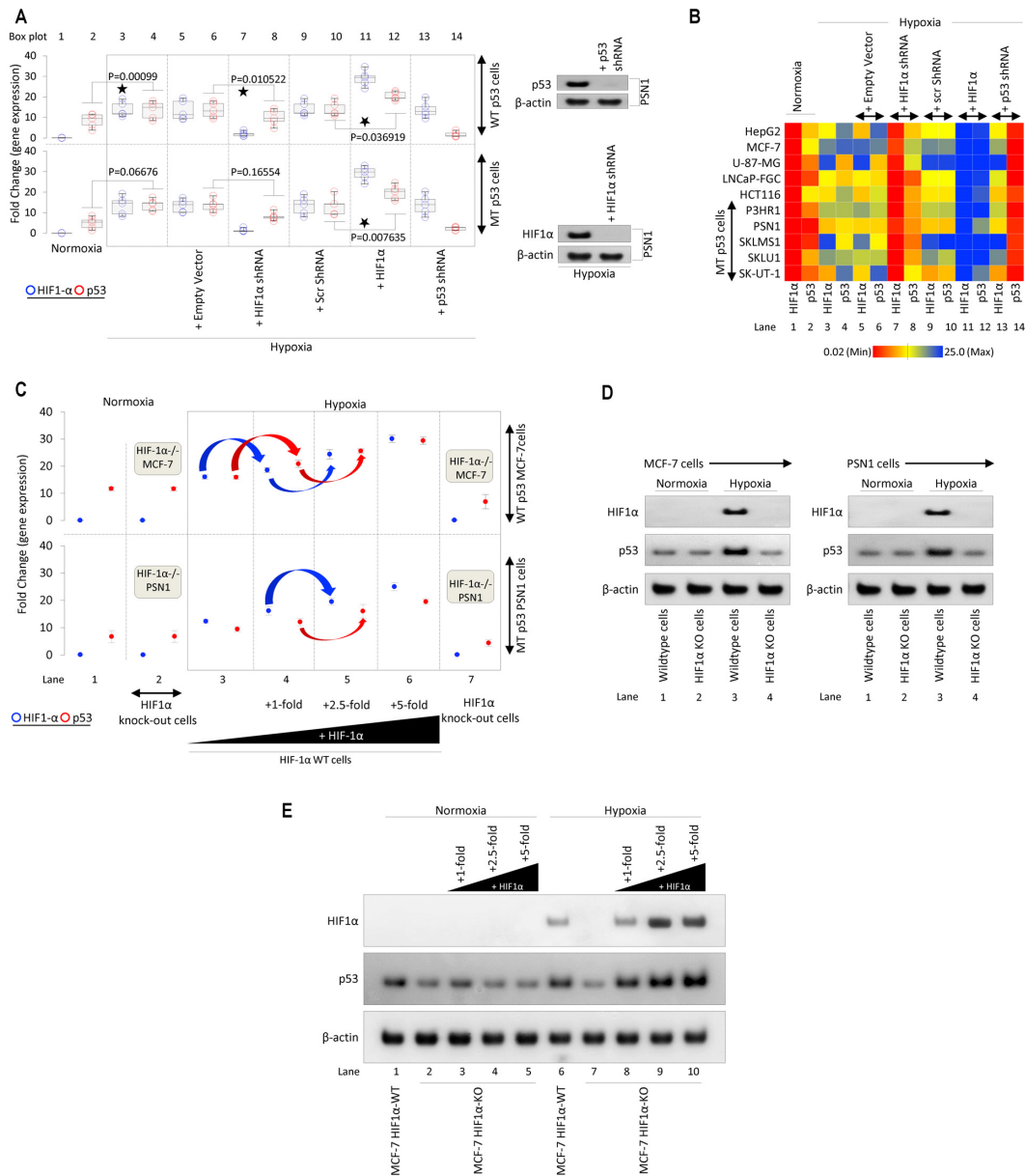
Figure 3. Genetic manipulation of HIF-1α affects p53 expression. (**A**) Effect of *HIF-1α* on *p53* expression in knockdown and overexpression experiments was observed using qRT-PCR in five *p53* WT and five *p53* MT cell lines (listed in 3B). Empty vector, *HIF-1α*-shRNA, non-specific Scr-shRNA, *HIF-1α*, or *p53*-shRNA were transfected in normoxic or hypoxic (1.8% O_2) cultured cells for 24 hrs. Hypoxia-induced expression of *p53* was abolished by *HIF-1α*-shRNA and increased upon exogenous addition of *HIF-1α*. For each cell line, gene expression was analyzed on three independent replicates (*n* = 5, per *p53* WT or MT *p53* cell lines). Inset: Western blot analysis confirms the effective knockdown of *p53* and *HIF-1α* in PSN1 cells. Two-sided Student's *t*-test was used for analysis; all *P* values are labeled on the figure. (**B**) Heat map depicts *p53* and *HIF-1α* gene expression under normoxia and hypoxia for each WT *p53* and MT *p53* cancer cell line (quantified in 3A). Results confirm effective knockdown of *p53* in by *p53*-shRNA, knockdown of *HIF-1α* by *HIF-1α*-shRNA, upregulation of *HIF-1α* by exogenous addition. Hypoxia-induced expression of WT or MT *p53* was dependent on *HIF-1α* levels. In this figure, each block represents the values from a gradient scale of low (red), medium (yellow) and high (blue) level of expression (*n* = 3). (**C**) Effect of *HIF-1α* knockdown and overexpression on *p53* expression was observed by qRT-PCR in WT and *HIF-1α* KO [MCF-7 (WT *p53*) and PSN-1 (MT *p53*)] hypoxic and normoxic cells. Crispr-generated *HIF-1α* null MCF-7 and PSN1 cells show no *HIF-1α* expression in normoxic and hypoxic cells (2 and 7). In hypoxic WT *HIF-1α* MCF-7 and PSN1 cells (panel 3–6), a consistent increase in *p53* expression is observed with a dose-dependent increase in *HIF-1α* expression. All hypoxic cells were cultured for 24 h in 1.8% O_2, *n* = 3, error bars represent SD. (**D**) Western blot analysis of whole-cell extracts from *HIF-1α*-WT MCF-7 or PSN1 and Crispr-generated *HIF-1α*$^{-/-}$ MCF-7 and PSN1 cells cultured under normoxia or hypoxia (at 1.8%O_2) for 24 h (*n* = 3 independent replicates). HIF-1α protein was absent in all cell lines under normoxia and increased in hypoxic *HIF-1α*-WT cells, but not *HIF-1α*$^{-/-}$ cells (top panel). Hypoxia resulted in increased p53 expression in *HIF-1α*-WT cells, however, in hypoxic *HIF-1α*$^{-/-}$ cells, depleted of HIF-1 α protein, p53 protein does not increase compared to normoxic *HIF-1α*$^{-/-}$ cells (middle panel). β-actin was used as a loading control. (**E**) Western blot analysis of HIF-1α and p53 was performed using whole-cell extracts from *HIF-1α* WT and *HIF-1α*$^{-/-}$ MCF-7 cells treated with or without increasing amounts of *HIF-1α* and cultured under normoxia or hypoxia (at 1.8%O_2) for 24 h (*n* = 3 independent replicates). HIF-1α and p53 protein increase in hypoxia-treated WT MCF-7 cells compared to normoxia. In *HIF-1α*$^{-/-}$ cells, hypoxia does not induce HIF-1α, and no significant increase in p53 is observed compared to normoxia (lane 7 versus lane 2). Exogenous addition of *HIF-1α* to hypoxic *HIF-1α*$^{-/-}$ cells restores HIF-1α expression and results in robust p53 induction in *HIF-1 α* dose-dependent manner (lanes 8–10). β-actin was used as the loading control.
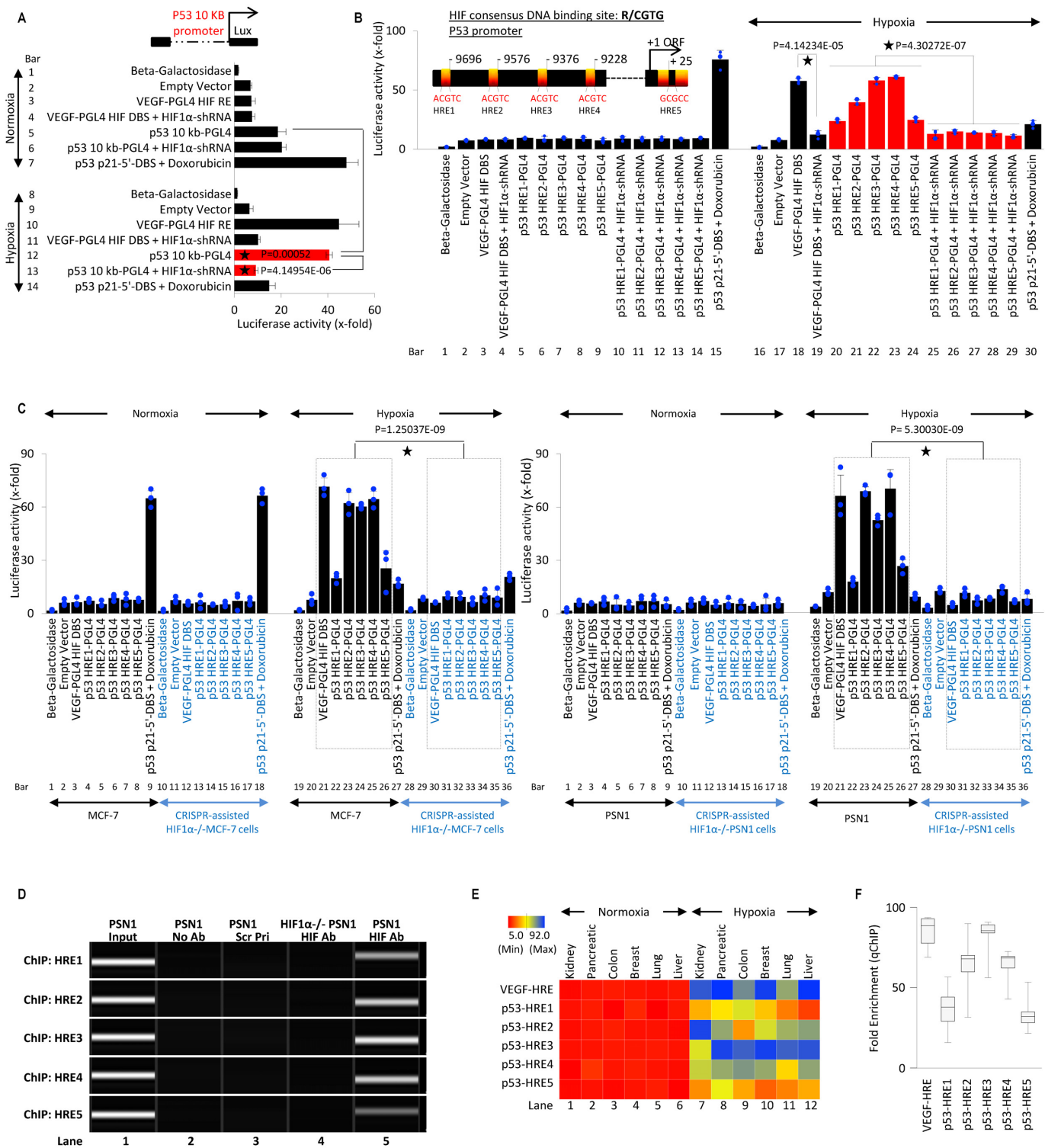
Figure 4. HIF-1α transcriptionally regulates p53. (**A**) Luciferase assay was used to determine hypoxia-induced and HIF-1α-dependent activation of full-length *p53* (10kb) promoter, a known HRE in *VEGF* promoter was cloned in PGL4 promoter and used as a positive control. Normoxia and hypoxia *p53* WT MCF-7 cells were transfected with *VEGF*-PGL4-HRE or *p53* 10kb-PGL4 alone or co-transfected with *HIF-1α*-shRNA under and harvested for luciferase assay. A known p53 DBS in *p21* promoter, p53 *p21*–5′-DBS-pGL4 was used as a positive control in doxorubicin-treated normoxic MCF-7 cells. Empty vector or Beta-galactosidase (β-Gal) served as normalization controls; error bars represent S.D., *n* = 3. Two-sided Student's *t*-test was used for analysis; all *P* values are labeled on the figure. (**B**) Luciferase assay was used to assess the activity of 5 putative HREs in the *p53* promoter, as depicted in the model. *p53* WT MCF-7 normoxic and hypoxic cells were transfected with *VEGF*-PGL4 vector, as a positive control for HIF-1α activity, or each *p53*-HRE-PGL4 vectors with or without *HIF-1α*-shRNA. Doxo-treated MCF-7 positive cells transfected with p53 *p21*-5′-DBS-pGL4 vector serves as positive control under normoxic conditions. The five *p53*-HREs sites display hypoxia-inducible luciferase activity that is blocked by shRNA-mediated *HIF-1α*

is required for *p53* transcription. As described previously (8,11,63), *p53* attains a transcriptionally inactive mutant-like conformation under hypoxic conditions. Similarly, we found that under doxorubicin treatment, p53-dependent activity at p53-regulated *p21* 5′DBS in was significantly reduced (bar 14); this data is further explained in Figure 5. Collectively, these results suggested that HIF-1α transcriptionally regulates *p53* promoter. To further determine elements of this HIF-1α-mediated p53 regulation, consensus HIF-1α REs (R/CGTG) in *p53* promoter were identified using Genomatix tool (99). Five HREs with 100% matching with template HRE sequence were found spanning across *p53* promoter, and their locations are depicted in a model (Figure 4B).

Individual HREs (HRE1–5) were cloned in the pGL4 promoter, and their activity was observed in WT *p53* MCF-7 cells. Data showed that all HREs in the *p53* promoter region, along with well-known *VEGF* promoter HRE were inactive in normoxic conditions (bars 3–9). Under hypoxia, the *VEGF* promoter (positive control) showed a significant increase in its promoter activity, which was reversed upon addition of *HIF-1α* shRNA (Figure 4B, bar 18 & 19). The newly identified five HREs in *p53* promoter also showed significant HIF-1α-dependent increase in their activity, which was reversed upon *HIF-1α* silencing (bars 20–29). To further identify this phenomenon in WT and MT *p53* cell lines (MCF7 and PSN1) under stricter genetic regulation (Crispr-assisted *HIF-1α* null cells), the activity of these five HREs in *p53* promoter was analyzed (Figure 4C). Under hypoxic conditions, *VEGF* HRE and five *p53* HREs were active in HIF-1α expressing MCF7 and PSN1 cells (bars 21–26). This activity of the HIF-1α-regulated elements in control (*VEGF*) and experimental *p53* HREs was reversed in *HIF-1α* null MCF7 and PSN1 cells. Given that *p53* promoter activity under hypoxia appeared to be *HIF-1α*-dependent, we next determined whether this regulation was the result of direct HIF-1α binding to the *p53* promoter at the five predicted HREs. We performed chromatin immuno-precipitation (ChIP) assay in *HIF-1α*⁺/⁺ (*HIF-1α* WT) and *HIF-1α*⁻/⁻ (*HIF-1α* KO) PSN1 cells which showed effective binding of HIF-1α on all five *p53* HREs (Figure 4D, lane 5). Significant HIF-1α binding to these five *p53* HREs was also observed by qChIP from the hypoxic regions of human kidney, pancreatic, colon, breast, lung and liver tumors ($n = 3$) (Figure 4E and F). As expected, no occupancy by HIF-1α occurred on any *p53*-HRE in normoxic regions of these tumors; however, a significant enrichment of these HREs was observed in all human tumor samples. Individual samples (Figure 4E) or collective binding affinity analysis (Figure 4F) revealed an exceptionally high affinity of HIF-1α toward HRE-2, 3 and 4. Since *VEGF* is a very active and high-affinity HRE, it was used as a positive control to compare HIF-1α affinity towards HREs in *p53* promoter.

Both WT and MT P53 binds to HIF-1α

Our results establish that HIF-1α transcriptionally induces the expression of p53. This finding has important biological significance because HIF-1α (pro-tumorigenic) and p53 (tumor suppressor) are known to induce opposite biological effects. We and others in the past have demonstrated that p53 is rendered transcriptionally inactive under physiological hypoxia (8,11,63). Despite this inactive conformation, p53 (both wild-type and mutant forms) which carries an intrinsically disordered N-terminus domain (100,88), might exert its effects via protein-protein interactions. We next investigated any potential hypoxia-stimulated p53 and HIF-1α protein interactions in molecular settings. Immunoprecipitation (IPP) was performed using anti-p53 ab and anti-HIF-1α ab in *HIF-1α*⁺/⁺, *HIF-1α*⁻/⁻, *p53*⁻/⁻, and double-*HIF-1α*⁻/⁻/ *p53*⁻/⁻ MCF-7 and PSN1 cells. IPP and development with the anti-HIF-1α showed the presence of bands in WT and *p53*⁻/- cells, and HIF-1α bands were missing in *HIF-1α*⁻/⁻ and double-*HIF-1α*⁻/⁻/ p53⁻/⁻ cells (Figure 5A, top left blot). IPP with anti-HIF-1α and development with anti-p53 ab shows the presence of bands in only WT cells, providing evidence that HIF-1α binds to both WT p53 (MCF-7) and MT p53 (PSN1) forms. Because of the absence of HIF-1α in lanes 2 and 4, and p53 in lane 3, no bands were observed. Next, IPP and development with anti-p53 ab showed bands in WT and *HIF-1α* KO MCF-7 and PSN1 cells. To cross-check the HIF-1α-p53 interaction, IPP was performed using anti-p53 ab and developed using anti-HIF-1α ab, which showed bands in only WT cells, (lane 1, bottom right blot). We further determined if HIF-1α-p53 interaction occurs in human cancers. Nuclear fraction (NF) from the hypoxic zones of prostate, breast, kidney, lung, colon, liver, ovarian and pancreatic cancer samples were collected and, (a) IPP with anti-p53 and development with anti-HIF-1α and (b) IPP with anti-HIF-1α ab and develop-

---

knockdown. Empty vector or Beta-galactosidase (β-Gal) served as normalization controls; error bars represent S.D., $n = 3$. Two-sided Student's *t*-test was used for analysis; all *P* values are labeled on the figure. (**C**) Luciferase assay was used to assess the 5 HREs in *p53* promoter under normoxia and hypoxia in *HIF-1α*-WT/KO MCF-7 and PSN1 cells. All cells were treated as described in (**B**) and harvested for luciferase assay. In both *HIF1-α*-WT MCF-7 (WT *p53*) and PSN1 (MT *p53*) cell lines, hypoxia leads to robust *p53* promoter activity at each HRE (lanes 22–26, left and right panel) compared to normoxia. Hypoxic induction of HRE promoter activity is lost in *HIF-1α*⁻/⁻ MCF-7 and PSN1 cells (lanes 31–35, left and right panel), indicating hypoxic induction of *p53* promoter activity is HIF-1α-dependent. Empty vector or Beta-galactosidase (β-Gal) served as normalization controls; error bars represent S.D., $n = 3$. Two-sided Student's *t*-test was used for analysis; all *P* values are labeled on the figure. (**D**) The ChIP-PCR assay was used to determine if HIF-1α binds to the five predicted HREs in *p53* promoter in hypoxic WT PSN1 and *HIF-1α*⁻/⁻ PSN1 cells. Lane 1: chromatin input. Lane 2: No Antibody negative control. Lane 3: a scrambled primer (Scr Pri) as a control for non-specific DNA PCR amplification. Lane 4: *HIF-1α*⁻/⁻ cells as a negative control for HIF-1α protein binding. Lane 5: binding of HIF-1α protein to each of the 5 HREs is observed, $n = 3$. (**E**) Heat map depicts HIF-1α binding to the 5 HREs in *p53* promoter measured by ChIP-qPCR in normoxic and hypoxic regions of kidney, pancreatic, colon, breast, lung and liver patient tumors. ChIP for HIF-1α binding to the *VEGF*-HRE was included as a positive control to confirm HIF-1α activation and binding activity. Variable HIF-1α binding to *p53*-HREs was detected in hypoxic regions, but not normoxic regions, from all cancer types. In this figure, each block represents the values from a gradient scale of low (red), medium (yellow), and high (blue) level of expression, $n = 3$ (biological replicates). (**F**) Box plot summary of ChIP-qPCR enrichment for each HRE in cancer hypoxic regions as described in (E). Fold enrichment depicts HIF-1α binding to *VEGF*-HRE or HRE 1–5 in *p53* promoter, in the hypoxic regions relative to HIF-1α binding in the normoxic regions, error bars represent S.D., $n = 3$.
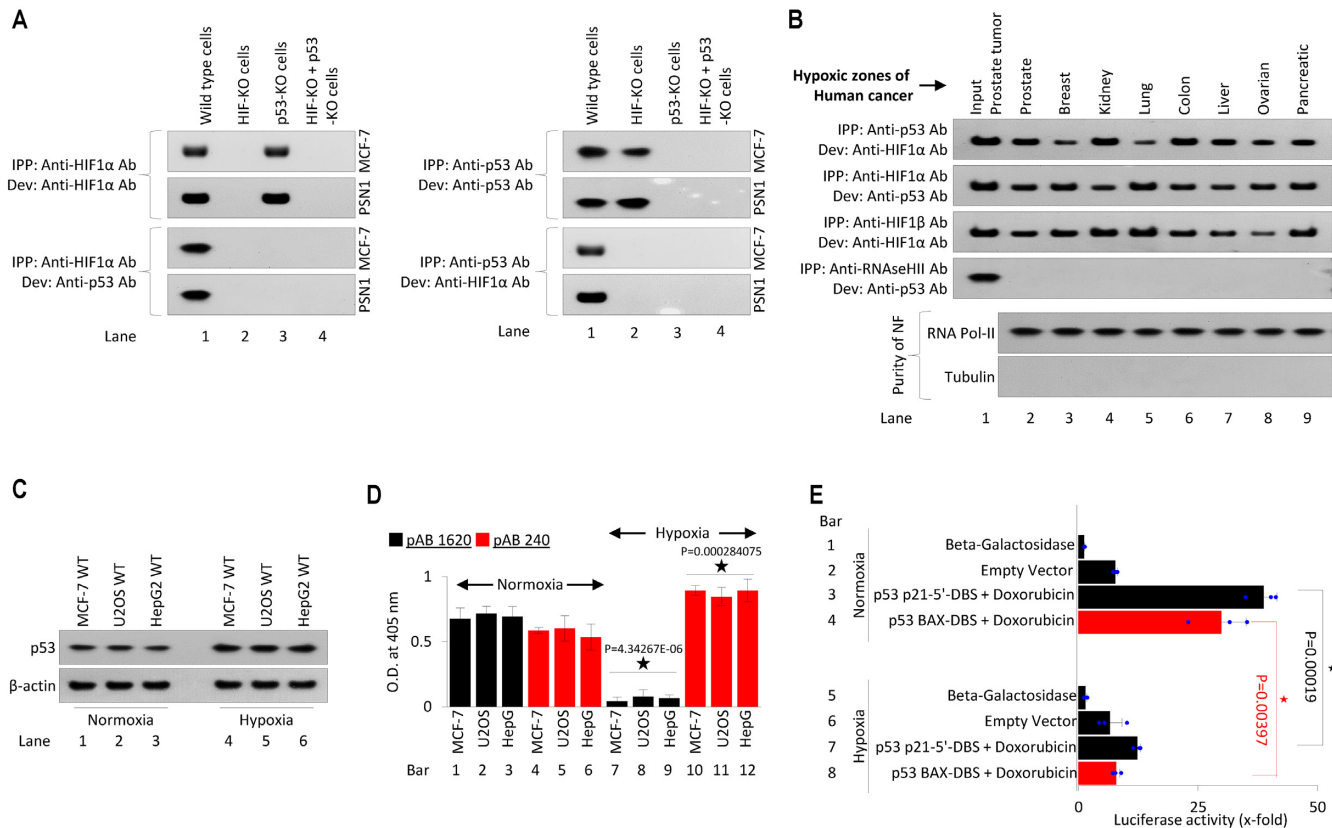
Figure 5. Both MT and WT p53 binds to HIF-1α. (**A**) Left panels: Immunoprecipitation (IPP) assay of endogenous HIF-1α from the nuclear fraction of hypoxia-treated *HIF-1α* and *p53* WT MCF7, *HIF-1α* WT and *p53* MT PSN1 cells, *HIF-1α* KO MCF7 and PSN1 cells (Crispr-assisted) and *HIF-1α* and *p53*-double KO MCF7 and PSN1 cells (Crispr-assisted). The top two panels are developed with Anti-HIF-1α Ab. The bottom two panels are developed with Anti-p53 Ab. Both HIF-1α and p53 bands are observed in WT cells of MCF-7 and PSN1 origin (first lane). No bands are observed in *HIF-1α* KO cells as IPP was performed using anti-HIF-1α Ab (lane 2). In *p53* KO cells bands were observed IPP and development were performed using anti-HIF-1α Ab, and no bands were detected when IPP was performed using anti-HIF-1α Ab and development was performed using anti-p53 Ab (lane 3). In lane 4, no bands were observed as *HIF-1α,* and *p53* double KO cells are used, and IPP is performed using anti-HIF-1α Ab. In the right panel: identical cell lines are used, but here the IPP is performed using anti-p53 Ab. In lane 1 bands are observed with development with both anti-p53 and anti-HIF-1α Abs. In lane 2 bands are observed in top 2 blots where p53 is IPPed and developed within *HIF-1α* KO cells, but when blots are developed with anti-HIF-1α Ab, these bands disappear. In lane 3 and 4, no bands are observed in *p53* KO, and *HIF-1α* and *p53* double KO cells as IPP is performed using anti-p53 Ab, $n = 3$. (**B**) Immunoprecipitation (IPP) assay of endogenous p53 and HIF-1α using the nuclear fraction (NF) from hypoxic tissue regions of 8 human cancers. In the first blot, IPP was performed against anti-p53 Ab and developed for HIF-1α protein; in second blot IPP was performed against anti-HIF-1α Ab and developed for p53 protein. HIF-1α and p53 were found to co-precipitate with each other in all hypoxic human cancer samples. In the third blot, all IPPs against HIF-1α show a positive signal for HIF-1 α protein, confirming IPP efficiency and antibody accuracy. In the fourth blot, IPP against RNAseH-II, a protein with no known p53 interaction, and developed against p53 results in no positive p53 signal for all samples, indicating accurate pull-down and antibody specificity for p53 protein. Positive detection of RNA-Pol II and negative detection of Tubulin were used as a protein loading control and for confirmation for the purity of nuclear fraction, $n = 3$. (**C**) Western blot analysis of p53 expression was performed using normoxic and hypoxic (1.8% O$_2$ for 24 h) *p53* WT MCF-7-, U2OS- and HepG-2 cells. Hypoxia induces p53 expression in each of the cell lines compared to normoxia. β-actin was used as a loading control, $n = 3$. (**D**) *In vivo,* ELISA was conducted to observe conformation shift recognized by p53 Ab-1620 (p53 WT conformation) and p53 Ab-240 (p53 MT conformation). WT *p53* MCF-7, UOS2, and HepG2 cells were cultured under normoxia and hypoxia (1.8% O$_2$ for 24 h). Hypoxia resulted in the loss of p53 Ab-1620 ELISA signal and increased p53 Ab-240 signal, indicating that hypoxia converts p53 to attain a mutant-like conformation, error bars represent S.D., $n = 3$. Two-sided Student's *t*-test was used for analysis; all *P* values are labeled on the figure. (**E**) Luciferase assay was used to observed p53-mediated activation of its downstream *p21* and *Bax*-minimal promoters. The p53-DBS within the promoter of the *p21* and *Bax* genes, two known p53 gene targets, were cloned into the pGL4 vector. Normoxic and hypoxic doxorubicin-treated MCF-7 cells were transfected with p53 *p21*-5′-DBS-pGL4 vector and with p53 *Bax*-5′-DBS-pGL4 and then harvested for luciferase assay. p53-driven transcriptional activity was lost under hypoxic conditions. Empty vector or Beta-galactosidase (β-Gal) served as normalization controls; error bars represent S.D., $n = 3$. Two-sided Student's *t*-test was used for analysis; all *P* values are labeled on the figure.

ment with anti-p53, showed presence of bands, suggesting HIF-1α-p53 interaction in all cancer types. Interaction between HIF-1α and ARNT/HIF-1β was used as a positive control in all these cancers. IPP with an antibody against RNAseH-II, a protein that does not interact with p53, results in no positive p53 signal, confirming p53 IPP efficiency. The purity of the nuclear fractions from tumors was

checked using western blotting with RNA Pol-II and tubulin (Figure 5B). We further checked the status of the p53 and its molecular conformation and transcriptional activity in hypoxic cancer cells. Western blot analysis confirmed that p53 expression was induced in hypoxic MCF-7, U2OS, and HepG-2 cells (Figure 5C). *In vivo* ELISA (88) using p53 wildtype conformation recognizing ab 1620 and mu-

tant conformation recognizing ab 240 ([11](#)) confirmed that p53 loses its molecular conformation to the attain a mutant like form under hypoxia (Figure 5D). Also, luciferase assay using *p21*-p53 5′ DBS and *Bax*-p53 DBS in MCF-7 *p53* WT background confirmed that p53 loses its transcriptional activity under hypoxia (Figure 5E, compare bars 3 & 4 with bars 7 & 8).

p53 enhances binding of HIF at HREs

Next, we sought to determine the biological effects of p53-HIF-1α interactions upon HIF-1α transcriptional activity. The promoter activity of two well-known targets of HIF-1α, *VEGF,* and *EPO* genes, in the presence and absence of p53, was analyzed by luciferase assay (Figure 6A). In *p53*-WT MCF-7 cells, HIF-1α activity on *VEGF* and *EPO* HREs (lanes 3 & 4) was significantly reduced upon addition of *p53* shRNA (lanes 5 & 6). Further, in hypoxic MCF-7 *p53* KO cells, HIF-1α activity at *VEGF* and *EPO* HREs was substantially reduced (lane 9 & 10). Interestingly, the addition of both WT *p53* and MT *p53* in *p53*$^{-/-}$ MCF7 cells led to a significant increase in the transcription of both *VEGF* and *EPO* HREs (lane 11–14) compared to *p53*-WT MCF7 cells (Figure 6A). These results suggest since increased p53 led to an increase in HIF-1α transcription factor activity. Next, we investigated whether this was the result of increased HIF-1α binding to HREs within target genes. We performed ChIP against HIF-1α on *VEGF*- and *EPO*-HRE in hypoxic WT PSN1 (carrying MT *p53* (K132Q)) and PSN1 *p53*$^{-/-}$ cells. HIF-1α enrichment at both the *VEGF* and *EPO* promoter is significantly reduced in PSN1 *p53*$^{-/-}$ (Figure 6B, lane 4) compared to wildtype/parental PSN1 cells (lane 3). Addition of either WT *p53* or MT *p53* (R175H) to hypoxic *p53*$^{-/-}$ PSN1 cells resulted in a recovery of HIF-1α binding to *VEGF* and *EPO* HREs (lanes 5 & 6). To determine whether p53-regulated HIF-1α recruitment to HIF-1α-target genes potentiates HIF-1α transcriptional activity, we performed qChIP on HIF-1α binding sites within promoter regions of 15 well-known downstream genes ([86,101,102](#)) from genetically modified tumor xenografts and human cancer samples. Tumor xenografts of approximately 4-cm^3 volume were generated from *p53*-WT MCF-7 and HCT-116 cells, *p53*$^{-/-}$-MCF-7 and -HCT-116 cells, and MT *p53*-transfected *p53*$^{-/-}$ MCF-7 and HCT-116 cells. qChIP showed a significant drop in the binding of HIF-1α to its HREs in hypoxic zones of the *p53* null tumors (Figure 6C, lanes 3 & 4, left heat map), when compared with tumor xenografts carrying WT of MT *p53* (Figure 6C). Additionally, we checked the HIF-1α-positive hypoxic regions in primary biopsies (FFPE samples) collected from four kidney, three pancreatic and four colon cancers with low and high p53 expression as shown in Figure 1A and also in the inset at the bottom of Figure 6C. Hypoxic regions with high and low p53 expression were collected separately using FFPE block punches and processed for qChIP. qChIP using patient cancer samples showed that HIF-1α binding to its HREs significantly decreases in regions with low p53 expression compared to regions with high p53 expression, (Figure 6C, compare lane 7–16 with 17–26, middle heat map). qChIP for 15 HIF-1α downstream genes in WT *p53* (1 each) and MT *p53* (1 each) breast, colon, and

pancreatic cancers showed no significant difference in affinity of HIF-1α towards its HREs in the presence of either WT or MT *p53* (lanes 27–32). qPCR was performed to observe the expression of the same 15 genes in genetically manipulated tumor xenografts and human tumors. This was done to determine the outcome of p53-dependent regulation of HIF-1α affinity towards its HREs, and whether the differences in HRE enrichment translate into differences in mRNA expression of these genes. Consistent with qChIP data, qPCR showed a significant reduction in the expression of 15 HIF-1α-regulated genes in *p53*-null MCF-7 and HCT-116 tumors (data for both tumor xenografts are combined in the top graph of Figure 6D). Similarly, in hypoxic regions of kidney, pancreatic and colon cancer patient samples, mRNA expressions of these 15 genes were lower in regions where expression of p53 was lower (data for all three tumors are merged in the bottom graph of Figure 6D).

p53-HIF-1α complex interacts with HREs

Collectively, our results show that p53 binds to HIF-1α and increases HIF-1α transcriptional activity. We next determined if p53 interacts with HIF-1α while HIF-1α is engaged at its downstream HREs, i.e. if a p53-HIF-1α complex binds to HIF-1α downstream HREs. We performed ChIP against p53 and HIF-1α to determine binding at *VEGF* HRE in hypoxic HCT-116 WT cells (which carry WT *p53*), HCT-116 *p53* KO, MCF-7 WT cells (which carry WT *p53*) and A-431 WT cells (which carry MT *p53*) (Figure 7A). We found that HIF was bound to the *VEGF* HRE as expected in all cell lines tested (lane 6), and p53 was bound to the *VEGF* HRE in HCT-116, MCF-7, and A-431 cells but not in HCT-116 *p53* KO cells (lane 5). To determine whether the observed p53 binding requires HIF-1α presence, we conducted HIF-1α and p53 ChIP-PCR at the *VEGF* HRE using cells in which *HIF-1α* gene is silenced using *HIF-1α* shRNA in HCT-116, HCT-116 *p53* KO and A-431 cells or CRISPR-assisted *HIF-1α* KO cells (Figure 7A).

ChIP in *HIF-1α* KD and KO cells using anti-HIF-1α Ab on *VEGF* HRE showed lack of any band, which is expected because there is no HIF-1α in these cells to bind to *VEGF* HRE (lane 7). Interestingly, p53 ChIP using *HIF-1α* KD and *HIF-1α* KO cells reveals that the absence of *HIF-1α* abrogates the p53 binding to *VEGF* HRE (lane 8, compared to lane 5). These results indicate p53 does not bind to *VEGF* HRE directly but rather binds to HIF-1α which interacts with the HRE, and thus a HIF-1α-p53 complex is working in tandem to achieve HIF-1α-induced transcriptional activation of HIF downstream genes. To further confirm this observation, *p53* shRNA was used to knockdown p53 in HCT-116 WT and A-431 cells and *p53* KO MCF-7 and HCT-116 cells were used to ChIP with anti-p53 ab, which showed no band in any cell lines, owing to lack of *p53* expression (lane 9). However, ChIP using anti-HIF-1α ab showed binding of HIF-1α to *VEGF* HRE in all *p53* lacking lines, indicating that HIF-1α binding is not dependent on p53 presence (lane 10).

This phenomenon was also observed in the hypoxic regions of breast cancer samples carrying MT *p53* or WT *p53* (Figure 7A, second panel). ChIP against p53 and HIF at *VEGF* HRE in these human cancers showed that both
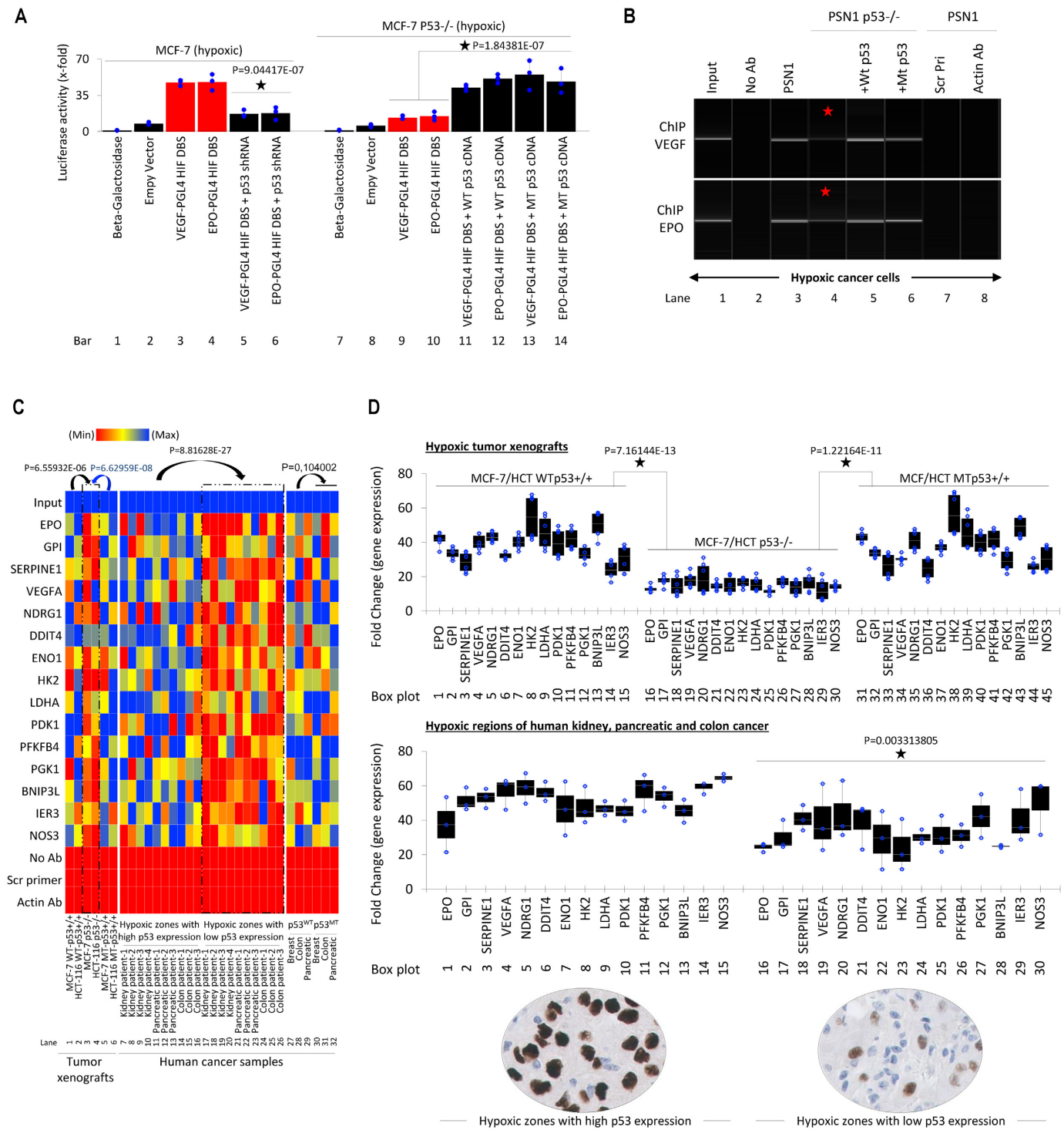
Figure 6. WT and MT *p53* enhance HIF-1α-dependent transcription and binding at HREs of downstream genes. (**A**) Luciferase activity was observed to study the impact of both WT and MT *p53* on HIF-1α-dependent transcription at the minimal promoters of its downstream genes *VEGF* and *EPO*. Hypoxic (1.8% O₂, 24 h) *p53* WT MCF7 and *p53* KO MCF7 cells were co-transfected with *VEGF*-PGL4 HRE or *EPO*-PGL4 HRE in the presence of *p53* shRNA, WT *p53* or MT *p53* and then harvested for luciferase assay. Loss of *p53* reduces HIF-1α-driven transcription at *VEGF* and *EPO* minimal promoters with HREs. Empty vector or Beta-galactosidase (β-Gal) served as normalization controls; error bars represent S.D., $n = 3$, Two-sided Student's *t*-test was used for analysis; all *P* values are labeled on the figure. (**B**) ChIP-PCR assay in hypoxia-treated *p53* WT PSN1 and *p53* KO PSN1 cells was performed to observe binding affinity of HIF-1α to the HREs in the *VEGF* and *EPO* promoters in presence and absence of WT and MT *p53*. Lane 1; 2% input was used, lane 2; no Antibody (Ab) was used as IP control, lane 7; Scrambled primers (scr pri) included as PCR amplification control, lane 8; actin Ab is used as a negative control. Data shows reduced enrichment of both *VEGF* and *EPO* promoters in *p53* KO PSN1 cells (lane 4) when compared to WT PSN1 cells (lane 3). Exogenous addition of WT *p53* (lane 5) and MT *p53* (lane 6) restores enrichment of HIF-1α at its HREs. (**C**) Heat map depicts qChIP assay demonstrating HIF-1α enrichment at the minimal promoters of 15 downstream genes, which are HIF targets with well-defined HREs. DNA

p53 and HIF-1α were present on the HRE, irrespective of *p53* genetic status. To again study the transcriptional activity and DNA binding capacity of p53 in hypoxic tumors and cancers (where it is itself transcriptionally inactive and attains a conformational mutant 240 form), p53-ChIP was performed on *Bax* p53-DBS, a well-characterized p53-target gene (93), in normoxic and hypoxic regions of both WT and MT p53-carrying breast cancers (Figure 7B). ChIP with anti-p53 ab in normoxic zones of breast cancer carrying WT p53 showed a positive interaction (top panel, lane 5). This interaction was lost in breast cancer carrying MT p53 and in hypoxic regions of both WT and MT p53-carrying breast cancers. The data suggest that p53 in hypoxic tumors again loses its molecular conformation to interact with DNA and thus cannot be present on *VEGF* HREs owing to DNA-protein interaction, but protein-protein interactions it shares with HIF-1α. A model explains how the p53-HIF-1α complex interacts with HRE (Figure 7C).

WT and MT p53 chaperone HIF-1α

The big question remains regarding the biological purpose of p53-HIF-1α complex binding to HIF downstream target genes. It is well known that hypoxia-induced stabilization of HIF-1α supports tumor growth by transcriptionally activating a myriad of genes that regulate important pro-cancer biological processes (15). Although p53 is commonly mutated in cancer, nearly 50% of human cancers contain wild-type p53. Despite the presence of wildtype p53 and its assumed pro-apoptotic activity, HIF-1α-induced pro-tumor activity is generally observed. Recent work has shown the pro-cancerous role of MT p53 and p53 in the hypoxic context (8,11,63). Thus, it is very unlikely that p53 binding destabilizes HIF-1α, rather it might be co-operating to stabilize HIF-1α. This possibility of p53-stabilized HIF-1α transcriptional activity is supported by our ChIP and qPCR data where the presence of WT and MT p53 both increase the affinity of HIF-1α towards its HREs, resulting in higher expression of its downstream genes. We determined if p53 binds to HIF-1α to chaperone and stabilize HIF-1α binding to the DNA and thus the synthesis of downstream genes. We designed an *in vivo* chaperone assay, as described previously (63). The molecular mechanism behind the assay is demon-

strated in the model in the inset (Figure 8A). The design includes co-transfection of a luciferase construct which carries 5 GAL-4 binding domains, followed by a *VEGF* HRE where HIF-1α can bind, along with fusion-protein expression constructs where GAL-4-p53 (MT/WT) proteins can be expressed in MCF-7 *p53* KO cells cultured under normoxia and hypoxic conditions. Because a free p53 molecule is present in the immediate vicinity of HIF-1α binding to its HRE, an interaction between p53 and HIF-1α at the *VEGF* HRE is forced. If p53 stabilizes and chaperones HIF-1α the luciferase activity at the *VEGF* HRE will increase. Data in bars 1, 2 and 11, 12, show experimental normalizing controls with empty PGL4 backbone and ß-galactosidase in normoxic and hypoxic MCF-7 p53 KO cells, respectively. In bars 3–9 (normoxic MCF-7 *p53* KO cells) and 13–19 (hypoxic MCF-7 *p53* KO cells), the GAL4-binding domain (repeated five times)-*VEGF* HRE-PGL4 vector is transfected. Under normoxic conditions (bars 3–9) because there is no HIF-1α expression, the HIF-1α-induced luciferase activity at the *VEGF* promoter is low. As a positive control in bar 10, p53 activity at a luciferase construct carrying p53 *p21* 5′DBS is observed in the presence of exogenous WT p53 and doxorubicin as a p53 activator. Important data is demonstrated in bars 13–19, where GAL4-binding domain (repeated five times)-*VEGF* HRE-PGL4 vector is transfected in hypoxic MCF-7 *p53* KO cells. A baseline reading is observed in bar 13 because HIF-1α is induced by hypoxia and drives transcription at the *VEGF* HRE; thus, a significant increase compared to bars 3–9 is observed. In bars 14 and 15, along with luciferase vector, a fusion protein expression vector which codes for GAL4 protein fused with C-terminus of WT or MT *p53* was transfected in hypoxic MCF-7 *p53* KO cells. Data showed a significant increase in HIF-1α-induced transcription at *VEGF* HRE, suggesting molecular chaperoning of HIF-1α by both MT and WT p53. To avoid the possibility of any contribution by GAL4-p53 fusion protein towards this increase in transcription, *HIF-1α* shRNA was added in combination with GAL4-MT/WT p53 protein in bars 16 and 17, which show a significant drop in HIF-1α-induced luciferase activity. Similar results were observed in hypoxic double *p53*-KO/*HIF-1α* KO MCF-7 cells transfected with GAL4-p53 fusion proteins in bars 18 and 19. The data confirm that the transcription at this

---

was harvested from *p53* WT MCF7, *p53* WT HCT-116, *p53* KO MCF7, MT *p53* MC7 and MT *p53* HCT116 cell line-derived xenografts grown in the flank region of the hind leg of nude mice. In addition, patient cancer samples from Kidney ($n = 4$), pancreatic ($n = 3$), and colon ($n = 3$) tumors characterized by high, or low *p53* expression were used. And finally, to observe if WT or MT *p53* impacts HIF-1α enrichment at HREs WT *p53* and MT *p53* breast, colon and pancreatic patient cancer samples were analyzed. Row 1; 2% input was used in all samples, row 17; no Antibody (Ab) included as IP control, row 18; Scrambled primers (Scr Pri) included as PCR amplification control and row 19; as non-specific anti-actin Ab as, negative control. In this figure, each block represents the values from a gradient scale of low (red), medium (yellow) and high (blue) level of expression. HIF-1α-enrichment is significantly lower in hypoxic *p53* null tumor xenografts (lane 3, 4), when compared with WT *p53* (lanes 1, 2) and MT *p53* (lanes 5, 6) tumor xenografts. In the patient samples hypoxic human tumors regions with high *p53* expression, show increased enrichment of HIF-1α on its downstream HREs (lane 7–16), when compared to regions with low *p53* expression (lanes 17–26). Finally, no significant difference in HIF-1α enrichment was observed between WT *p53* (lane 27–29) and MT *p53* (lane 30–32) tumor, $n = 3$. Two-sided Student's *t*-test was used for analysis; all *P* values are labeled on the figure. (**D**) Top panel: Expression of 15 HIF-regulated genes described in A, were analyzed by qRT-PCR in hypoxic regions *p53* WT MCF-7 and HCT-116, *p53*$^{-/-}$ MCF-7 and HCT-116, and MT *p53* expressing *p53*$^{-/-}$ MCF-7 and HCT-116 tumor xenografts. Loss of *p53* significantly reduced expression of all 15 genes. Data from MCF-7 and HCT tumors are pooled for analysis, $n = 3$, error bars represent S.D., $n = 3$. Two-sided Student's *t*-test was used for analysis; all *P* values are labeled on the figure. Bottom panel: Expression of these genes is observed in pooled samples from hypoxic regions of four kidney, three pancreatic and four colon tumors characterized by high and low *p53* expression (Inset below the plots). Reduced target gene expression was observed in hypoxic zones of cancers with low *p53* expression compared to hypoxic zones with high p53 expression. Data from tumors with high versus low *p53* expression is pooled for analysis, $n = 3$, error bars represent S.D., $n = 3$. Two-sided Student's *t*-test was used for analysis; all *P* values are labeled on the figure.
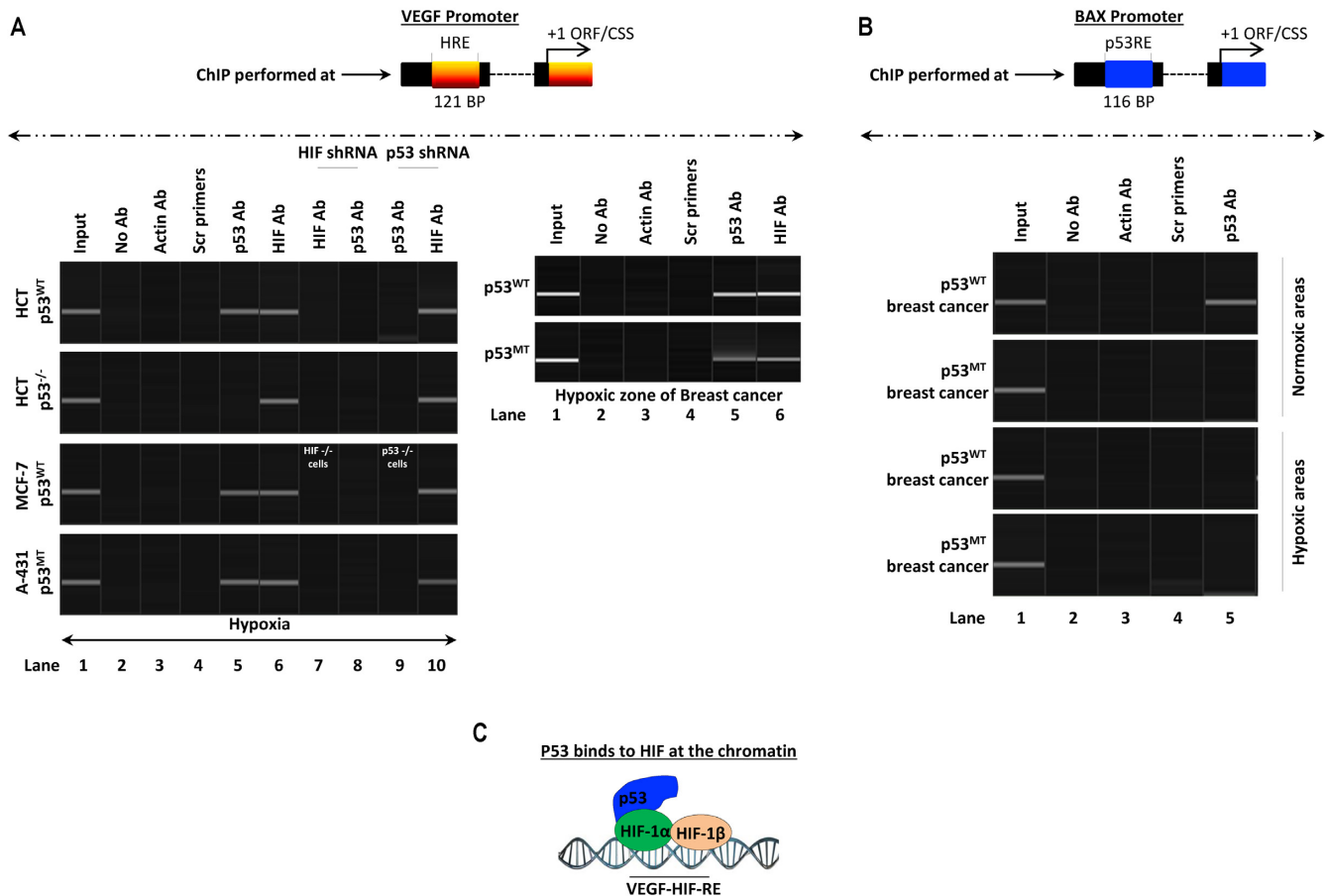
Figure 7. Both WT and MT p53 form a transcriptional complex with HIF-1α at HREs. (**A**) Left panel: ChIP-PCR assay to observe if p53-HIF-1α complex binds to HREs of HIF downstream genes such as *VEGF*. In a genetically controlled experiment, WT *p53* (HCT-116 and MCF-7), *p53* KO MCF-7 and MT *p53* A-431 cells were used. Lane 1; 2% input was used, lane 2; no Antibody (Ab) was used as IP control, lane 3; actin Ab is used as a negative control, lane 4; Scrambled primers (scr pri) included as PCR amplification control. ChIP with anti-p53 ab for HRE at *VEGF* minimal promoter gives a band in WT and MT *p53* cells, suggesting that p53 binds to hypoxia response element, lane 5. ChIP with anti-HIF-1α Ab shows bands in all cell types, lane 6. In lanes 7 and 8, *HIF-1α* KD and use of *HIF-1α* KO cells (MCF-7 origin), results in disappearance for bands for both HIF-1α and p53 Abs, suggesting that p53 does not bind directly to HREs but is present there because of its binding to HIF-1α. In lanes 9 and 10, use of *p53* shRNA or *p53* KO MCF-7 cells abolishes all bands for ChIP with anti-p53 Ab, but the bands for ChIP with anti-HIF-1α Ab are present, suggesting that p53 is not required for HIF-1α to bind to its HREs, $n = 3$. In the second panel: this binding of p53 to HIF-1α response elements is observed in WT and MT hypoxic breast tumors, bands are observed for both anti-p53 and anti-HIF-1α ChIP, lanes 5 and 6 respectively, suggesting that HIF-1α-p53 complex is functional during HIF-driven transcription in hypoxic human cancers, $n = 3$. (**B**) ChIP-PCR assay using Anti-p53 Ab to measure p53 binding to the p53 DBS in the *Bax* promoter from normoxic and hypoxic zones of *p53* WT and *p53* MT breast cancer patient samples. Lane 1; 2% input was used, lane 2; no Antibody (Ab) was used as IP control, lane 3; anti-actin Ab was used as a negative control for ChIP, and lane 4; scrambled primers (Scr Pri) included as PCR amplification control. In lane 5; the data show that p53 binds to *Bax* p53-DBS only in the presence of WT *p53* in normoxic tumors. In hypoxic tumors of any *p53* origin or normoxic MT *p53* tumors, this association is not observed, $n = 3$. (**C**) A model shows the mechanism where WT/MT p53 binds to HIF-1α and not to HREs directly.

GAL4-binding domain (repeated five times)-*VEGF* HRE-PGL4 vector is driven by HIF-1α and presence of MT/WT p53 in its immediate vicinity stabilizes HIF-1α and increases its transcriptional activity in this molecular chaperone assay. We next asked whether the transcriptional effects of the p53-HIF-1α complex were the result of altered HIF-1α protein stability. We performed cycloheximide chase to determine the effects of p53 on HIF-1α protein stability and found that exogenous addition of WT or MT p53 to MCF-7 p53-KO cells (Figure 8B, lanes 4–9) under hypoxia enhanced HIF-1α stability compared to controls (lanes 1–3). These results indicate that the formation of p53-HIF-1α complex protects HIF-1α against protein degradation. The statistical analysis and quantification of the cycloheximide chase experiment is presented (Figure 8C).

Chaperoning of HIF-1α by WT and MT p53 increases HIF transcriptional ability

The molecular chaperone assay establishes that p53 can stabilize and promote HIF-1α-induced transcription in cellular conditions, we observed if this phenomenon holds true for *in vitro* transcription (Figure 9A). An *in vitro* transcription cassette was designed as shown previously (85,91,92), six *VEGF* HREs were repeated to ensure robust HIF binding, followed by AdML core promoter followed by a start codon of a G-less cassette followed by a Poly-A tail. The RNA-Pol II machinery and required transcription factor HIF and molecular chaperone p53 were obtained from nuclear extracts of MCF-7 *HIF-1α* KO, *p53* KO, and double *HIF-1α p53* KO cells, and the readout of the assay was
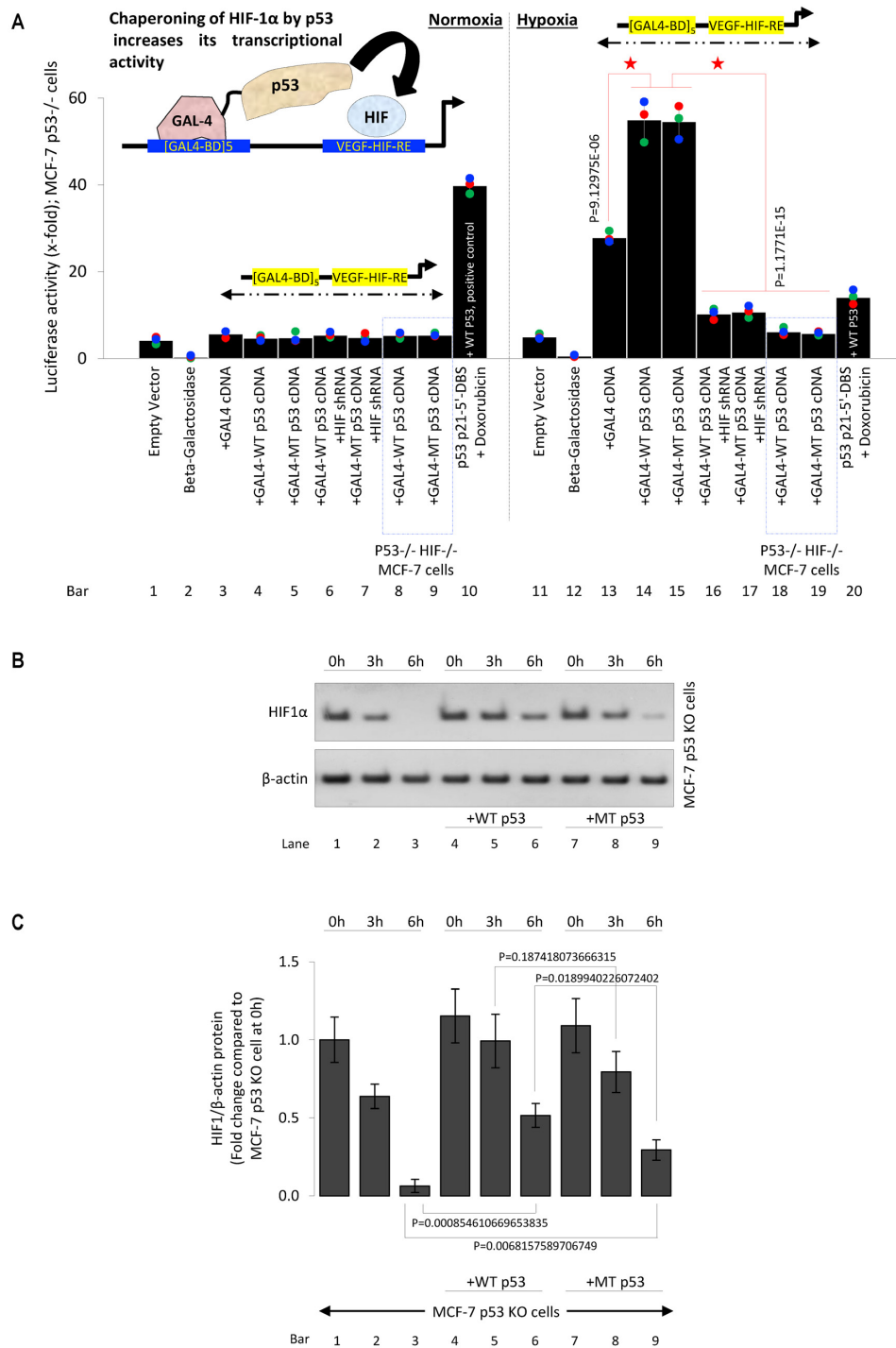
Figure 8. Hypoxic WT & MT p53 chaperones HIF-1α at chromatin. (**A**) *In vivo* Chaperone Assay to measure the ability of WT or MT p53 to chaperone HIF-1α. The output read of this chaperone assay is the increase HIF-1α-driven transcription at its downstream *VEGF* HRE. *p53*$^{-/-}$ MCF7 or *p53* and *HIF-1α* double KO MCF-7 cells were co-transfected with [GAL4-BD]₅-*VEGF*-HRE luciferase construct together with GAL4, WT *p53*-GAL4, MT *p53*-GAL4 alone or in combination with *HIF-1α* shRNA. In the left panel, this HIF-driven construct shows no activity in normoxia-cultured cells (lane-3–9), p53-driven *p21* luciferase vector in doxorubicin-treated cells, is used as a positive control in normoxia (lane 10). Under hypoxic conditions, a baseline activity of the HIF-1α-driven *VEGF* promoter is observed (lane 13). Interestingly presence of WT p53 (lane 14) or MT p53 (lane 15) as chaperone increases HIF-1α-driven transcription; this effect is lost upon addition of *HIF-1α* shRNA or in *HIF-1α* KO cells (lane16–19). Empty vector or Beta-galactosidase (β-Gal) served as normalization controls; error bars represent S.D., $n = 3$. Two-sided Student's *t*-test was used for analysis; all *P* values are labeled on the figure. (**B**) Western blot analysis of cycloheximide chase to study the effects of p53 expression on HIF-1α protein stability. *p53* KO MCF-7 cells and *p53* KO MCF-7 cells transfected with WT *p53* or MT *p53* were cultured under hypoxia for 24 h and treated with cycloheximide (100 μg/ml) for indicated times. HIF-1α protein is degraded within 6 h in *p53* KO cells (lane 3), but both WT and MT p53 protect HIF-1 α against protein degradation (lanes 6 and 9). (**C**) Statistical analysis and quantification of the HIF-1α protein expression during the cycloheximide chase experiment shown in Figure 8B is presented. Error bars represent S.D., $n = 3$. Two-sided Student's *t*-test was used for analysis; all *P* values are labeled on the figure.
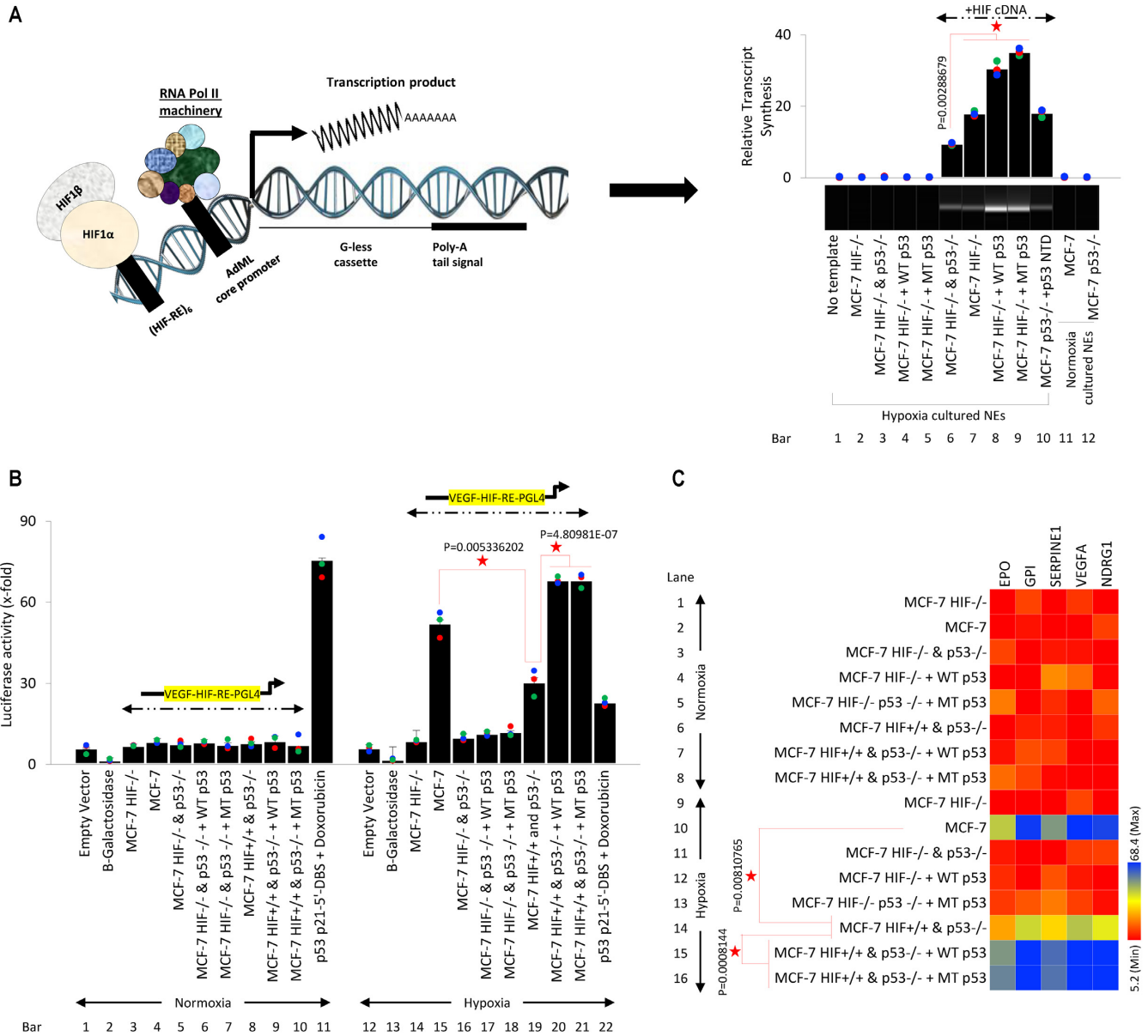
Figure 9. Chaperoning of HIF-1α by WT & MT p53 promotes HIF-1 transcriptional activity. (**A**) *In vitro* transcription assay was performed using a cassette designed with six *VEGF* HRE repeats, followed by AdML core promoter, start codon of a G-less cassette and Poly-A tail. The RNA-Poll machinery and required transcription factor HIF-1α and molecular chaperone p53 were obtained from nuclear extracts of MCF-7 *HIF-1α* KO, *p53* KO, and double *HIF-1α p53* KO cells, and the readout of the assay was obtained by qPCR and by QIAXEL. In lane 1 no DNA template is added (negative control). No signal is observed where HIF-1α is lacking, lane 2–5. A signal is observed in from nuclear extract of MCF-7 *HIF-1α* and *p53* double KO exogenously transfected with *HIF-1α* (lane 6), which is further amplified by rescuing WT or MT p53 expression (lanes 7–9). Exogenous addition of p53 N-terminus (A.A. 1–125) also rescues HIF-1α-driven transcription (lane 10). No signal is observed from normoxic cells because they lack HIF-1α expression (lane 11–12). Error bars represent S.D., $n = 3$. Two-sided Student's *t*-test was used for analysis; all *P* values are labeled on the figure. (**B**) Effects of chaperone assay and *in vitro* transcription are observed in cellular conditions. Luciferase assay was performed on normoxic and hypoxic MCF-7 cells of different genetic backgrounds transfected with PGL4 luciferase vector with a *VEGF* HRE. Under hypoxia, cells carrying WT *HIF-1α* and WT *p53* show a significant increase in *VEGF* HRE activity that is inhibited by loss of *HIF-1α* or *p53* and augmented by overexpression of WT or MT *p53*. Error bars represent S.D., $n = 3$. Two-sided Student's *t*-test was used for analysis; all *P* values are labeled on the figure. (**C**) The effects of *HIF-1α* and *p53* genetic manipulation were tested on a panel of 5 HIF-1α downstream genes, *EPO, GPI, SERPINE1, VEGFA*, and *NDRG1*. Genetically manipulated normoxic or hypoxic MCF-7 cells were used for qRT-PCR analysis. Heat map depicts the gene expression of HIF-1α target genes. HIF-1α-regulated genes are poorly expressed under normoxia and highly induced by hypoxia plus overexpression of WT or MT *p53* in *HIF*$^{+/+}$; *p53*$^{-/-}$ cells. p53-induced upregulation of HIF-1α target genes is diminished by concurrent HIF-1α deficiency. In this figure, each block represents the values from a gradient scale of low (red), medium (yellow) and high (blue) level of expression, $n = 3$. Two-sided Student's *t*-test was used for analysis; all *P* values are labeled on the figure.

obtained by qPCR and by QIAXEL. A series of controls were run. In lane 1, bar 1 the *in vitro* transcription template was not added, and thus no signal was observed. In lane 2, bar 2 the template was added, but the MCF-7 *HIF-1α* KO nuclear extract was used, which again resulted in no signal. In lane 3, bar 3 nuclear extract from MCF-7 *HIF-1α* and *p53* double KO was used. In lane 4, bar 4 and lane 5, bar 5 nuclear extracts from MCF-7 *HIF-1α* KO cells transfected with WT *p53* and MT *p53* were used, because *HIF-1α* is lacking in all these nuclear extracts no signal was observed. In lane 6, bar 6 nuclear extract from MCF-7 *HIF-1α* and *p53* double KO exogenously transfected with *HIF-1α* was used, because *HIF-1α* was present in this extract a signal was observed, this also served as a positive control for the experiment. Next, the nuclear extract of MCF-7 *HIF-1α* KO cells which carry WT *p53*, transfected with *HIF-1α* was used, which resulted in a significant increase in HIF-1α transcriptional activity (lane 7, bar 7). To observe this p53-induced increase in HIF-1α transcriptional activity, nuclear extract from MCF-7 *HIF-1α* KO cells transfected with WT *p53* and MT *p53* was used in lane 8, bar 8 and lane 9, bar 9 respectively. A significant increase in the HIF-1α-induced transcription was observed in the presence of both MT and WT *p53*. In lane 10, bar 10 the nuclear extract from MCF-7 *p53* KO cells transfected with *HIF-1α* and *p53* NTD (N-terminus domain, amino acid 1–125) was used as a control of p53 chaperoning activity, based on purported chaperoning abilities of p53 NTD (63). In lane 11, bar 11 and lane 12, bar 12 nuclear extracts from normoxic MCF-7 WT cells and MCF-7 *p53* KO cells were used, which resulted in no signal, suggesting that p53 does not influence this transcription in the absence of HIF-1α. Since the *in vitro* transcription data support the findings of the molecular chaperone assay, next we determined to see the same this identical *in vitro* transcription panel in cellular conditions using luciferase assay (Figure 9B). Normoxic and hypoxic MCF-7 cells of different genetic backgrounds were transfected with PGL4 luciferase vector with a *VEGF* HRE. In the left panel bars 1–10, because of lack of HIF-1α in normoxic cells luciferase activity at *VEGF* HRE is low, in bar 11, a positive control is used where MCF-7 cells were transfected with p53 *p21* 5′DBS in the presence of doxorubicin. In hypoxic cells, bars 12 and 13 served as normalization controls with empty vector and ß-Galactosidase. In bar 14, MCF-7 *HIF-1α* KO cells show a lack of activity, whereas, in bar 15, WT MCF-7 cells carrying *HIF-1α* and WT *p53* show a significant increase in *VEGF* HRE activity. This activity is reversed in MCF-7 *HIF-1α* and *p53* double KO cells (bar 16), and double KO cells in the presence of WT *p53* (bar 17) and MT *p53* (bar 18). In bar 19, MCF-7 *p53* KO cells which carry *HIF-1α* show an increase in activity, but lower than WT MCF-7 cells which carry WT *p53* (bar 15). Addition of WT and MT *p53* in MCF-7 *p53* KO cells, bars 20 and 21, respectively, results in a significant increase in HIF-1α-induced activity at *VEGF* HRE. Bar 22 shows reduced transcriptional activity of p53 on *p21* 5′DBS in hypoxic cells when compared to bar 11. Next, we analyzed the impact of this panel on HIF-1α-induced expression of its five downstream genes, *EPO, GPI, SERPINE1, VEGFA* and *NDRG1* with qPCR in genetically manipulated hypoxic and normoxic MCF-7 cells (Figure 9C). In lane 1–8, because the cells were cultured in

normoxic conditions, expression of most of these HIF-1α-regulated genes is poor. In lane 9, 11, 12 and 13 hypoxic MCF-7 *HIF-1α* KO or *HIF-1α* and *p53* double KO cells show poor expression of these genes, most likely because of lack of *HIF-1α*. In WT MCF-7 cells which carry *HIF-1α* and WT *p53* expression of these genes is significantly increased (lane 10). However, in *p53* KO MCF-7 cells expression of these genes is significantly reduced (lane 14), this reduction is reversed upon exogenous addition of WT *p53* (lane 15) and MT *p53* (lane 16). All the data from molecular chaperone assay, *in vitro* transcription, *in vivo* luciferase assay and qPCR assay in a consistent panel of normoxic and hypoxic MCF-7, MCF-7 *HIF-1α* KO, MCF-7 *p53* KO and MCF-7 *HIF-1α* and *p53* double KO cells, establish the fact that p53 chaperones and stabilizes HIF-1α while it binds to HREs of its downstream genes, resulting in more efficient transcription and thus advanced pro-tumor activity.

DISCUSSION

Here, we have discovered a novel feedback loop operational between p53 and HIF-1α. With the help of non-invasive O_2 measurements in human tumor xenografts using electron paramagnetic resonance, we made considerable effort to identify and simulate physiologically relevant oxygen conditions (∼1.8% O_2). This unique feedback loop is observed upon hypoxia-induced activation of HIF-1α, which binds to its response elements on the *p53* promoter and results in upregulation of both WT and MT p53 proteins depending on *p53* genetic status. The p53 transcriptional activity under hypoxic conditions is compromised, and both genetic WT and MT p53 attains a conformational mutant phenotype. This upregulated p53 protein binds and chaperones HIF-1α, which results in increased binding and affinity of HIF towards the response elements (REs) of its downstream genes. Thus, p53-assisted HIF-1α chaperoning increases efficiency of HIF to function as a pro-cancer transcription factor. HIF-1α-p53 (MT/WT) complex is found binding at specific HRE of HIF downstream genes and supports the fact that hypoxic tumors where p53 and HIF-1α both are upregulated are associated with a worse prognosis. A model in Figure 10 summarizes these findings.

HIF-induced p53 upregulation has been previously reported in both WT p53 (13), and MT p53 (60) cells and a positive correlation between the expression of p53 and HIF-1α was observed (59,103). However, this study presents an in-depth analysis in hypoxic regions of solid tumors to establish the relationship between p53 and HIF-1α mRNA and protein expression in a variety of tumors. Our results with ChIP and luciferase assay demonstrate that *p53* promoter is under HIF regulation, which transcriptionally induces the synthesis of both WT and MT p53. Consensus hypoxia response elements R/CGTG within p53 promoter were identified to be enriched with HIF-1α, providing concrete answers to the question of whether HIF-1α induces expression of p53 and it upregulates MT or WT p53, as was observed previously (56,57,104–106). We and others have consistently found that p53 is transcriptionally compromised in hypoxic cells, and some groups found that it can only function as a trans-repressor (63,64,107). Here and in our previous studies, we have shown that both WT and
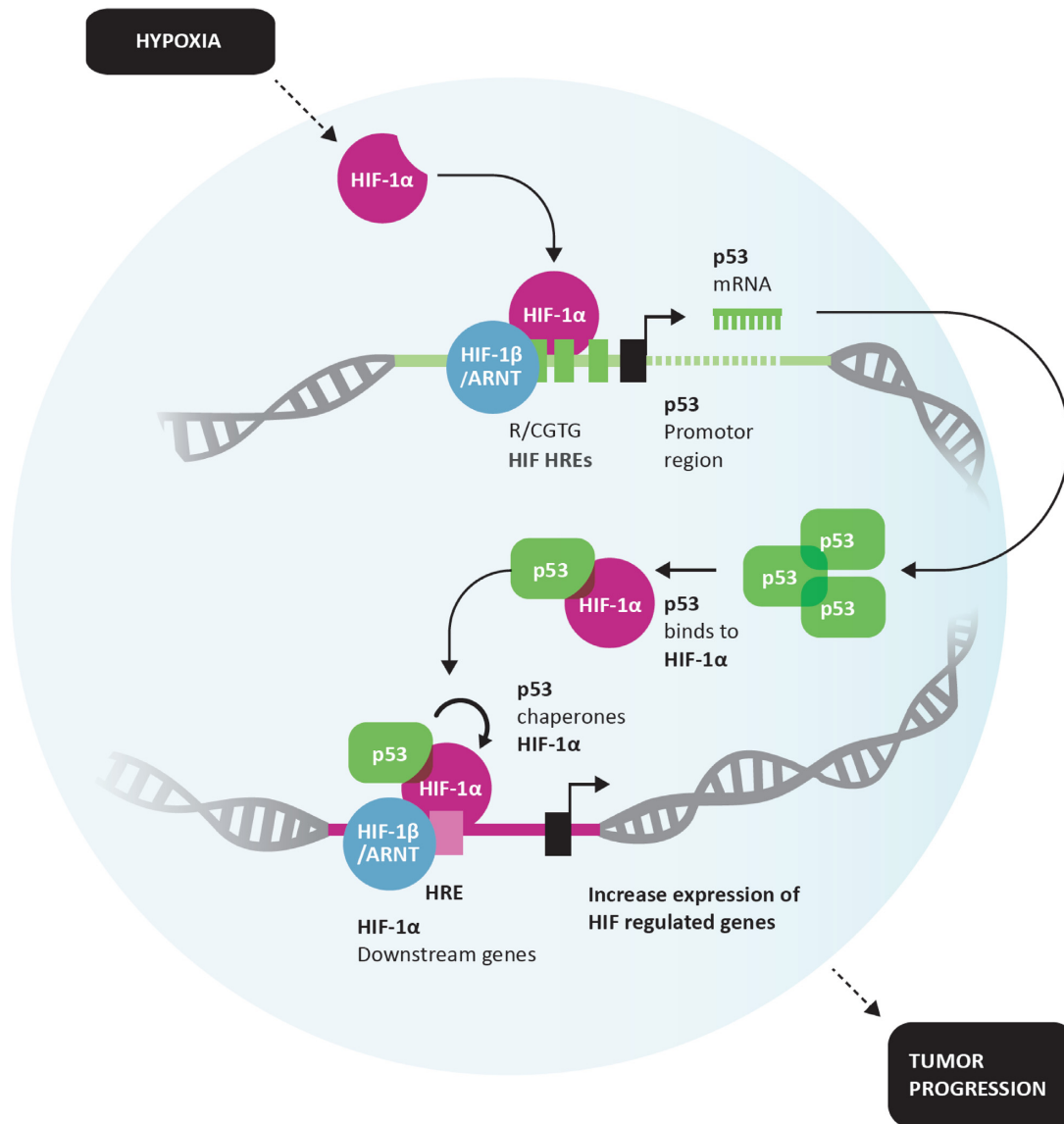
Figure 10. Model depiction: Positive feedback loop between HIF-1α and p53 drives HIF-1α downstream signaling. Hypoxia-stimulated HIF-1α binds to HREs within *p53* promoter and increases *p53* transcription resulting in p53 protein accumulation. Under hypoxia, p53 may obtain a MT conformation. Both MT and WT p53 bind to HIF-1α protects HIF-1 α against protein degradation and chaperones HIF-1α toward the response elements of target genes, increasing transcriptional activity. Ultimately, p53-chaperoning of HIF-1 α under hypoxia exacerbates HIF-1 α signaling, fueling the pro-tumorigenic properties of HIF-1α.

MT *p53* genetic mutants under hypoxic conditions adopt a transcriptionally inactive mutant-like protein conformation recognized by pAB 240 instead of pAB 1620 (11).

Binding between WT/MT p53 and HIF-1α under *in vitro* and *in vivo* conditions has been shown previously (61,62,108), but the question still remained whether WT or MT p53 or both can bind to HIF-1α in hypoxic cells. p53 is intrinsically disordered at its N- and C-terminus and stable in its core domain and is known to interact with many proteins, such as CBP/p300, CSN5/Jab1, Mdm2, RPA, TFIID, 14–3-3, GSK3β, hGcn5, PARP-1, S100B(ββ), TAF, TAF1, TRRAP, TFIIH, along with HIF-1α and many other proteins, clearly illustrating exceptional binding promiscuity of p53 (109). Thus p53-HIF-1α inter-

action in its upregulated levels is easy to understand. We further show evidence of p53-HIF-1α binding in Crispr-assisted *p53* null, *HIF-1α* null, and *p53+HIF-1α* nulls cells with WT *p53* carrying MCF-7 cells and MT *p53* carrying PSN1 cells. A recent study demonstrated the ability of HIF-1α to bind to MT p53 proteins (such as p53 R273H and p53 R246I) with compromised p53-DNA interactions (60), whereas our results indicate that this interaction is universal and occurs with WT p53 and a large variety of p53 mutants. We further observed that the HIF-1α-p53 complex together binds to the DNA response elements of HIF downstream genes. At HIF-response elements, p53 does not directly interact with DNA but rather binds to and chaperones HIF-1α. A similar observation was also recently made

(60), with the exception that not only MT p53 but also WT p53 demonstrate similar nature of interactions with HIF-1α.

In this study for the first time, we demonstrate that both WT and MT p53 can serve as a molecular chaperone and stabilize HIF-1α. We have used cutting-edge molecular design for developing an *in vivo* chaperone assay and *in vitro* transcription assay to establish that both MT and WT p53 chaperones and stabilizes HIF-1α and promotes HIF-1α-induced transcription at hypoxia DNA response elements. This results in an increased efficiency of HIF-1α to upregulate expression of its downstream genes involved in regulation of important biological processes such as, but not limited to, glucose uptake (20,21), metabolism (22–24), angiogenesis (25,26), erythropoiesis (27), cell proliferation (28), differentiation (29), and apoptosis (30). Recently, it was suggested that HIF-1α forms a protein complex exclusively with MT p53, and this complex is also found at the chromatin (60). Our ChIP results on HIF-regulated REs suggest that both WT and MT p53 form complex with HIF-1α, and this complex directly interact with the DNA elements. It is important to note that p53 does not directly bind to HREs. Recent reports suggest that MT p53 assists HIF-1α in activating hypoxia-regulated genes because it recruits an SWI/SNF chromatin remodeling complex and it is the presence of SWI/SNF which facilitates activation of a specific subset of genes such as the ECM components type VIIa1 collagen and laminin-γ2 (60). Our data identify that relation between both WT/MT p53 and HIF-1α is more direct, where the both WT/MT p53 can chaperone HIF-1α directly while in a complex at the chromatin, this chaperoning stabilizes HIF-1α-HRE interactions and globally improves synthesis of HIF-downstream genes involved in cell survival, angiogenesis, and regulation of metabolism, etc., and are not limited to ECM components.

Here, we have presented definitive evidence of a unique physiological situation under which WT p53 can function as a tumor promoter by its chaperone activity towards HIF-1α, previously, the pro-cancerous role of MT p53 was discovered (109–111). This finding demonstrates the dual role of p53 has great implications and showcases the complexity of p53 signaling given that p53 may function as a tumor-suppressor in normoxic regions (a transcriptional mechanism) and as a tumor-promoter (chaperone for HIF-1α) in hypoxic regions of the same tumor.

The finding that both WT and MT p53 bind and chaperone HIF-1α is very important because no hypoxia-associated disease model other than cancer is known to harbor p53 mutations and carry WT *p53* genotype, thus WT p53-HIF-1α specific interactions can drive similar molecular effects in other hypoxia-associated diseases. Therefore, this finding also has implications beyond cancer in other hypoxic disease models such as chronic inflammatory bowel disease, rheumatoid arthritis, and ischemia/reperfusion injury, cystic fibrosis, chronic bronchitis, stroke, psoriasis, diabetic vasculopathy, and epilepsy. In human disease pathophysiology, alteration of HIF-1α activity prominently affects vascularization in ischemia (i.e., myocardial, cerebral, retinal), hypertension, and tumor progression. Chronic overexpression of HIF-1α is witnessed in patients with Von Hippel-Lindau (VHL) syndrome, a genetic disease affecting blood vessel growth that is characterized by increased tumor formation (112). VHL tumor suppressor is an E3 ubiquitin ligase that targets alpha subunits of HIFs for proteasomal degradation under normoxic conditions (113). Loss of VHL creates a pseudo hypoxic environment leading to HIF stabilization (112). VHL-deficient carcinoma cells are shown to overproduce direct HIF targets, *VEGF, GLUT1, PDGF-B,* and *CXCR4* (112,114,115). On the other end of the spectrum, HIF-1α abrogation produces opposing effects. Complete deficiency of HIF-1α causes embryonic lethality in *Hif1a⁻/⁻* mice owing to cardiac and vascular malformations (116). Chronic hypoxia treatment of wild-type mice leads to the development of polycythemia, right ventricular hypertrophy, pulmonary hypertension, and pulmonary vascular remodeling, all of which are delayed by partial HIF-1α deficiency in *HIF1a⁺/⁻* mice (117). Conditional and tissue-specific manipulation of VHL/HIF-1α pathway reveals pivotal roles in osteogenesis (118), pancreatic beta-cell insulin secretion (119), myeloid cell-mediated inflammation (120), and development of the sympathetic nervous system (121). A significant threat to cardiovascular health is cardiac ischemia and subsequent hypertrophy. In a mouse model of pressure overload, HIF-1α activation initially promoted vascular growth in the heart by inducing angiogenic factors (122). However, sustained pressure overload led to p53 accumulation and HIF-1α inhibition, causing a transition from cardiac hypertrophy toward heart failure (122). This newly discovered HIF-1α and p53 relationship in light of these disease models is critical in understanding and explaining peculiar clinical findings and observations.

REFERENCES

1. Simon,M.C. and Keith,B. (2008) The role of oxygen availability in embryonic development and stem cell function. *Nat. Rev. Mol. Cell Biol.*, **9**, 285–296.
2. Giaccia,A.J., Simon,M.C. and Johnson,R. (2004) The biology of hypoxia: the role of oxygen sensing in development, normal function, and disease. *Genes Dev.*, **18**, 2183–2194.
3. Semenza,G.L. (2001) Hypoxia-inducible factor 1: control of oxygen homeostasis in health and disease. *Pediatr. Res.*, **49**, 614–617.

4. Hong,W.X., Hu,M.S., Esquivel,M., Liang,G.Y., Rennert,R.C., McArdle,A., Paik,K.J., Duscher,D., Gurtner,G.C., Lorenz,H.P. *et al.* (2014) The role of Hypoxia-Inducible factor in wound healing. *Adv. Wound Care (New Rochelle)*, **3**, 390–399.

5. Ruthenborg,R.J., Ban,J.J., Wazir,A., Takeda,N. and Kim,J.W. (2014) Regulation of wound healing and fibrosis by hypoxia and hypoxia-inducible factor-1. *Mol. Cells*, **37**, 637–643.

6. Bell,S.L. and Eveson,D.J. (2011) An unusual cause of stroke and hypoxia. *BMJ*, **342**, c7200.

7. Ferdinand,P. and Roffe,C. (2016) Hypoxia after stroke: a review of experimental and clinical evidence. *Exp. Transl. Stroke Med.*, **8**, 9.

8. Achison,M. and Hupp,T.R. (2003) Hypoxia attenuates the p53 response to cellular damage. *Oncogene*, **22**, 3431–3440.

9. Deben,C., Deschoolmeester,V., De Waele,J., Jacobs,J., Van den Bossche,J., Wouters,A., Peeters,M., Rolfo,C., Smits,E., Lardon,F. *et al.* (2018) Hypoxia-Induced cisplatin resistance in Non-Small cell lung cancer cells is mediated by HIF-1 alpha and Mutant p53 and can be overcome by induction of oxidative stress. *Cancers*, **10**, E126.

10. Goda,N., Ryan,H.E., Khadivi,B., McNulty,W., Rickert,R.C. and Johnson,R.S. (2003) Hypoxia-inducible factor 1 alpha is essential for cell cycle arrest during hypoxia. *Mol. Cell Biol.*, **23**, 359–369.

11. Gogna,R., Madan,E., Kuppusamy,P. and Pati,U. (2012) Re-oxygenation causes hypoxic tumor regression through restoration of p53 wild-type conformation and post-translational modifications. *Cell Death Dis.*, **3**, e286.

12. Graeber,T.G., Osmanian,C., Jacks,T., Housman,D.E., Koch,C.J., Lowe,S.W. and Giaccia,A.J. (1996) Hypoxia-mediated selection of cells with diminished apoptotic potential in solid tumours. *Nature*, **379**, 88–91.

13. Hammond,E.M., Denko,N.C., Dorie,M.J., Abraham,R.T. and Giaccia,A.J. (2002) Hypoxia links ATR and p53 through replication arrest. *Mol. Cell Biol.*, **22**, 1834–1843.

14. Hockel,M., Schlenger,K., Hockel,S. and Vaupel,P. (1999) Hypoxic cervical cancers with low apoptotic index are highly aggressive. *Cancer Res.*, **59**, 4525–4528.

15. LaGory,E.L. and Giaccia,A.J. (2016) The ever-expanding role of HIF in tumour and stromal biology. *Nat. Cell Biol.*, **18**, 356–365.

16. Oh,S.Y., Kwon,H.C., Kim,S.H., Jang,J.S., Kim,M.C., Kim,K.H., Han,J.Y., Kim,C.O., Kim,S.J., Jeong,J.S. *et al.* (2008) Clinicopathologic significance of HIF-1alpha, p53, and VEGF expression and preoperative serum VEGF level in gastric cancer. *BMC Cancer*, **8**, 123.

17. Singh,D., Arora,R., Kaur,P., Singh,B., Mannan,R. and Arora,S. (2017) Overexpression of hypoxia-inducible factor and metabolic pathways: possible targets of cancer. *Cell Biosci.*, **7**, 62–70.

18. Welford,S.M. and Giaccia,A.J. (2011) Hypoxia and Senescence: The impact of oxygenation on tumor suppression. *Mol Cancer Res.*, **9**, 538–544.

19. Yamamoto,Y., Ibusuki,M., Okumura,Y., Kawasoe,T., Kai,K., Iyama,K. and Iwase,H. (2008) Hypoxia-inducible factor 1 alpha is closely linked to an aggressive phenotype in breast cancer. *Breast Cancer Res. Trans.*, **110**, 465–475.

20. Denko,N.C. (2008) Hypoxia, HIF1 and glucose metabolism in the solid tumour. *Nat. Rev. Cancer*, **8**, 705–713.

21. Eales,K.L., Hollinshead,K.E. and Tennant,D.A. (2016) Hypoxia and metabolic adaptation of cancer cells. *Oncogenesis*, **5**, e190.

22. Brahimi-Horn,M.C., Chiche,J. and Pouyssegur,J. (2007) Hypoxia signalling controls metabolic demand. *Curr. Opin. Cell Biol.*, **19**, 223–229.

23. Rajendran,J.G., Mankoff,D.A., O'Sullivan,F., Peterson,L.M., Schwartz,D.L., Conrad,E.U., Spence,A.M., Muzi,M., Farwell,D.G. and Krohn,K.A. (2004) Hypoxia and glucose metabolism in malignant tumors: evaluation by [18F]fluoromisonidazole and [18F]fluorodeoxyglucose positron emission tomography imaging. *Clin. Cancer Res.*, **10**, 2245–2252.

24. Kim,J.W., Tchernyshyov,I., Semenza,G.L. and Dang,C.V. (2006) HIF-1-mediated expression of pyruvate dehydrogenase kinase: a metabolic switch required for cellular adaptation to hypoxia. *Cell Metab*, **3**, 177–185.

25. Ozawa,K., Kondo,T., Hori,O., Kitao,Y., Stern,D.M., Eisenmenger,W., Ogawa,S. and Ohshima,T. (2001) Expression of the oxygen-regulated protein ORP150 accelerates wound healing by modulating intracellular VEGF transport. *J. Clin. Invest.*, **108**, 41–50.

26. Liao,D. and Johnson,R.S. (2007) Hypoxia: a key regulator of angiogenesis in cancer. *Cancer Metastasis Rev.*, **26**, 281–290.

27. Haase,V.H. (2010) Hypoxic regulation of erythropoiesis and iron metabolism. *Am. J. Physiol. Renal. Physiol.*, **299**, F1–F13.

28. Hubbi,M.E. and Semenza,G.L. (2015) Regulation of cell proliferation by hypoxia-inducible factors. *Am. J. Physiol. Cell Physiol.*, **309**, C775–C782.

29. Zhu,L.L., Wu,L.Y., Yew,D.T. and Fan,M. (2005) Effects of hypoxia on the proliferation and differentiation of NSCs. *Mol. Neurobiol.*, **31**, 231–242.

30. Semenza,G.L. (2012) Hypoxia-inducible factors in physiology and medicine. *Cell*, **148**, 399–408.

31. Chan,M.C., Holt-Martyn,J.P., Schofield,C.J. and Ratcliffe,P.J. (2016) Pharmacological targeting of the HIF hydroxylases–A new field in medicine development. *Mol. Aspects Med.*, **47-48**, 54–75.

32. Kung,A.L., Zabludoff,S.D., France,D.S., Freedman,S.J., Tanner,E.A., Vieira,A., Cornell-Kennon,S., Lee,J., Wang,B., Wang,J. *et al.* (2004) Small molecule blockade of transcriptional coactivation of the hypoxia-inducible factor pathway. *Cancer Cell*, **6**, 33–43.

33. Semenza,G.L. (2012) Hypoxia-inducible factors: mediators of cancer progression and targets for cancer therapy. *Trends Pharmacol. Sci.*, **33**, 207–214.

34. Jaakkola,P., Mole,D.R., Tian,Y.M., Wilson,M.I., Gielbert,J., Gaskell,S.J., von Kriegsheim,A., Hebestreit,H.F., Mukherji,M., Schofield,C.J. *et al.* (2001) Targeting of HIF-alpha to the von Hippel-Lindau ubiquitylation complex by O2-regulated prolyl hydroxylation. *Science*, **292**, 468–472.

35. Semenza,G.L. (2003) Targeting HIF-1 for cancer therapy. *Nat. Rev. Cancer*, **3**, 721–732.

36. Jiang,B.H., Semenza,G.L., Bauer,C. and Marti,H.H. (1996) Hypoxia-inducible factor 1 levels vary exponentially over a physiologically relevant range of O2 tension. *Am. J. Physiol.*, **271**, C1172–C1180.

37. Graham,A.M. and Presnell,J.S. (2017) Hypoxia Inducible Factor (HIF) transcription factor family expansion, diversification, divergence and selection in eukaryotes. *PLoS One*, **12**, e0179545.

38. Semenza,G.L. and Wang,G.L. (1992) A nuclear factor induced by hypoxia via de novo protein synthesis binds to the human erythropoietin gene enhancer at a site required for transcriptional activation. *Mol. Cell Biol.*, **12**, 5447–5454.

39. Gu,Y.Z., Moran,S.M., Hogenesch,J.B., Wartman,L. and Bradfield,C.A. (1998) Molecular characterization and chromosomal localization of a third alpha-class hypoxia inducible factor subunit, HIF3alpha. *Gene Expr.*, **7**, 205–213.

40. Koh,M.Y., Lemos,R. Jr., Liu,X. and Powis,G. (2011) The hypoxia-associated factor switches cells from HIF-1alpha- to HIF-2alpha-dependent signaling promoting stem cell characteristics, aggressive tumor growth and invasion. *Cancer Res.*, **71**, 4015–4027.

41. Obacz,J., Pastorekova,S., Vojtesek,B. and Hrstka,R. (2013) Cross-talk between HIF and p53 as mediators of molecular responses to physiological and genotoxic stresses. *Mol. Cancer*, **12**, 93–102.

42. Marin-Hernandez,A., Gallardo-Perez,J.C., Ralph,S.J., Rodriguez-Enriquez,S. and Moreno-Sanchez,R. (2009) HIF-1alpha modulates energy metabolism in cancer cells by inducing over-expression of specific glycolytic isoforms. *Mini Rev. Med. Chem.*, **9**, 1084–1101.

43. Bartoszewska,S., Kochan,K., Piotrowski,A., Kamysz,W., Ochocka,R.J., Collawn,J.F. and Bartoszewski,R. (2015) The hypoxia-inducible miR-429 regulates hypoxia-inducible factor-1alpha expression in human endothelial cells through a negative feedback loop. *FASEB J.*, **29**, 1467–1479.

44. Maynard,M.A., Evans,A.J., Shi,W., Kim,W.Y., Liu,F.F. and Ohh,M. (2007) Dominant-negative HIF-3 alpha 4 suppresses VHL-null renal cell carcinoma progression. *Cell Cycle*, **6**, 2810–2816.

45. Makino,Y., Cao,R., Svensson,K., Bertilsson,G., Asman,M., Tanaka,H., Cao,Y., Berkenstam,A. and Poellinger,L. (2001) Inhibitory PAS domain protein is a negative regulator of hypoxia-inducible gene expression. *Nature*, **414**, 550–554.

46. Vousden,K.H. and Lu,X. (2002) Live or let die: the cell's response to p53. *Nat. Rev. Cancer*, **2**, 594–604.

47. Yue,X., Zhao,Y., Xu,Y., Zheng,M., Feng,Z. and Hu,W. (2017) Mutant p53 in Cancer: Accumulation, Gain-of-Function, and Therapy. *J. Mol. Biol.*, **429**, 1595–1606.

48. Oren,M. and Rotter,V. (2010) Mutant p53 gain-of-function in cancer. *Cold Spring Harb. Perspect. Biol.*, **2**, a001107.

49. Milner,J. and Watson,J.V. (1990) Addition of fresh medium induces cell cycle and conformation changes in p53, a tumour suppressor protein. *Oncogene*, **5**, 1683–1690.

50. Zhang,W., Hu,G., Estey,E., Hester,J. and Deisseroth,A. (1992) Altered conformation of the p53 protein in myeloid leukemia cells and mitogen-stimulated normal blood cells. *Oncogene*, **7**, 1645–1647.

51. Bartek,J., Iggo,R., Gannon,J. and Lane,D.P. (1990) Genetic and immunochemical analysis of mutant p53 in human breast cancer cell lines. *Oncogene*, **5**, 893–899.

52. Xu,J., Reumers,J., Couceiro,J.R., De Smet,F., Gallardo,R., Rudyak,S., Cornelis,A., Rozenski,J., Zwolinska,A., Marine,J.C. *et al.* (2011) Gain of function of mutant p53 by coaggregation with multiple tumor suppressors. *Nat. Chem. Biol.*, **7**, 285–295.

53. Zhang,Y., Coillie,S.V., Fang,J.Y. and Xu,J. (2016) Gain of function of mutant p53: R282W on the peak? *Oncogenesis*, **5**, e196.

54. Hammond,E.M. and Giaccia,A.J. (2005) The role of p53 in hypoxia-induced apoptosis. *Biochem. Biophys. Res. Commun.*, **331**, 718–725.

55. Pan,Y., Oprysko,P.R., Asham,A.M., Koch,C.J. and Simon,M.C. (2004) p53 cannot be induced by hypoxia alone but responds to the hypoxic microenvironment. *Oncogene*, **23**, 4975–4983.

56. Sermeus,A. and Michiels,C. (2011) Reciprocal influence of the p53 and the hypoxic pathways. *Cell Death Dis.*, **2**, e164.

57. Fels,D.R. and Koumenis,C. (2005) HIF-1alpha and p53: the ODD couple? *Trends Biochem. Sci.*, **30**, 426–429.

58. Hammond,E.M. and Giaccia,A.J. (2006) Hypoxia-inducible factor-1 and p53: friends, acquaintances, or strangers? *Clin. Cancer Res.*, **12**, 5007–5009.

59. Sumiyoshi,Y., Kakeji,Y., Egashira,A., Mizokami,K., Orita,H. and Maehara,Y. (2006) Overexpression of hypoxia-inducible factor 1 alpha and p53 is a marker for an unfavorable prognosis in gastric cancer. *Clin. Cancer Res.*, **12**, 5112–5117.

60. Amelio,I., Mancini,M., Petrova,V., Cairns,R.A., Vikhreva,P., Nicolai,S., Marini,A., Antonov,A.A., Le Quesne,J., Baena Acevedo,J.D. *et al.* (2018) p53 mutants cooperate with HIF-1 in transcriptional regulation of extracellular matrix components to promote tumor progression. *Proc. Natl. Acad. Sci. U.S.A.*, **115**, E10869–E10878.

61. Hansson,L.O., Friedler,A., Freund,S., Rudiger,S. and Fersht,A.R. (2002) Two sequence motifs from HIF-1alpha bind to the DNA-binding site of p53. *Proc. Natl. Acad. Sci. U.S.A.*, **99**, 10305–10309.

62. Sanchez-Puig,N., Veprintsev,D.B. and Fersht,A.R. (2005) Binding of natively unfolded HIF-1alpha ODD domain to p53. *Mol. Cell*, **17**, 11–21.

63. Gogna,R., Madan,E., Kuppusamy,P. and Pati,U. (2012) Chaperoning of mutant p53 protein by wild-type p53 protein causes hypoxic tumor regression. *J. Biol. Chem.*, **287**, 2907–2914.

64. Koumenis,C., Alarcon,R., Hammond,E., Sutphin,P., Hoffman,W., Murphy,M., Derr,J., Taya,Y., Lowe,S.W., Kastan,M. *et al.* (2001) Regulation of p53 by hypoxia: Dissociation of transcriptional repression and apoptosis from p53-dependent transactivation. *Mol. Cell Biol.*, **21**, 1297–1310.

65. Soengas,M.S., Alarcon,R.M., Yoshida,H., Giaccia,A.J., Hakem,R., Mak,T.W. and Lowe,S.W. (1999) Apaf-1 and caspase-9 in p53-dependent apoptosis and tumor inhibition. *Science*, **284**, 156–159.

66. Hammond,E.M., Mandell,D.J., Salim,A., Krieg,A.J., Johnson,T.M., Shirazi,H.A., Attardi,L.D. and Giaccia,A.J. (2006) Genome-wide analysis of p53 under hypoxic conditions. *Mol. Cell Biol.*, **26**, 3492–3504.

67. Azhar,G., Liu,L., Zhang,X. and Wei,J.Y. (1999) Influence of age on hypoxia/reoxygenation-induced DNA fragmentation and bcl-2, bcl-xl, bax and fas in the rat heart and brain. *Mech. Ageing Dev.*, **112**, 5–25.

68. Chowdhury,A.R., Long,A., Fuchs,S.Y., Rustgi,A. and Avadhani,N.G. (2017) Mitochondrial stress-induced p53 attenuates HIF-1alpha activity by physical association and enhanced ubiquitination. *Oncogene*, **36**, 397–409.

69. Denko,N.C., Green,S.L., Edwards,D. and Giaccia,A.J. (2000) p53 checkpoint-defective cells are sensitive to X rays, but not hypoxia. *Exp. Cell Res.*, **258**, 82–91.

70. Tamatani,M., Mitsuda,N., Matsuzaki,H., Okado,H., Miyake,S., Vitek,M.P., Yamaguchi,A. and Tohyama,M. (2000) A pathway of neuronal apoptosis induced by hypoxia/reoxygenation: roles of nuclear factor-kappaB and Bcl-2. *J. Neurochem.*, **75**, 683–693.

71. Kim,C.Y., Tsai,M.H., Osmanian,C., Graeber,T.G., Lee,J.E., Giffard,R.G., DiPaolo,J.A., Peehl,D.M. and Giaccia,A.J. (1997) Selection of human cervical epithelial cells that possess reduced apoptotic potential to low-oxygen conditions. *Cancer Res.*, **57**, 4200–4204.

72. Muz,B., de la Puente,P., Azab,F. and Azab,A.K. (2015) The role of hypoxia in cancer progression, angiogenesis, metastasis, and resistance to therapy. *Hypoxia (Auckl)*, **3**, 83–92.

73. Petrova,V., Annicchiarico-Petruzzelli,M., Melino,G. and Amelio,I. (2018) The hypoxic tumour microenvironment. *Oncogenesis*, **7**, 10.

74. Hockel,M. and Vaupel,P. (2001) Tumor hypoxia: definitions and current clinical, biologic, and molecular aspects. *J. Natl. Cancer Inst.*, **93**, 266–276.

75. Rankin,E.B. and Giaccia,A.J. (2016) Hypoxic control of metastasis. *Science*, **352**, 175–180.

76. Wenger,R.H., Kurtcuoglu,V., Scholz,C.C., Marti,H.H. and Hoogewijs,D. (2015) Frequently asked questions in hypoxia research. *Hypoxia (Auckl)*, **3**, 35–43.

77. Vengellur,A. and LaPres,J.J. (2004) The role of hypoxia inducible factor 1alpha in cobalt chloride induced cell death in mouse embryonic fibroblasts. *Toxicol. Sci.*, **82**, 638–646.

78. Lopez-Sanchez,L.M., Jimenez,C., Valverde,A., Hernandez,V., Penarando,J., Martinez,A., Lopez-Pedrera,C., Munoz-Castaneda,J.R., De la Haba-Rodriguez,J.R., Aranda,E. *et al.* (2014) CoCl2, a mimic of hypoxia, induces formation of polyploid giant cells with stem characteristics in colon cancer. *PLoS One*, **9**, e99143.

79. Dai,Z.J., Gao,J., Ma,X.B., Yan,K., Liu,X.X., Kang,H.F., Ji,Z.Z., Guan,H.T. and Wang,X.J. (2012) Up-regulation of hypoxia inducible factor-1alpha by cobalt chloride correlates with proliferation and apoptosis in PC-2 cells. *J. Exp. Clin. Cancer Res.*, **31**, 28.

80. Guo,M., Song,L.P., Jiang,Y., Liu,W., Yu,Y. and Chen,G.Q. (2006) Hypoxia-mimetic agents desferrioxamine and cobalt chloride induce leukemic cell apoptosis through different hypoxia-inducible factor-1alpha independent mechanisms. *Apoptosis*, **11**, 67–77.

81. Klumpen,E., Hoffschroer,N., Zeis,B., Gigengack,U., Dohmen,E. and Paul,R.J. (2017) Reactive oxygen species (ROS) and the heat stress response of Daphnia pulex: ROS-mediated activation of hypoxia-inducible factor 1 (HIF-1) and heat shock factor 1 (HSF-1) and the clustered expression of stress genes. *Biol. Cell.*, **109**, 39–64.

82. Chi,J.T., Wang,Z., Nuyten,D.S., Rodriguez,E.H., Schaner,M.E., Salim,A., Wang,Y., Kristensen,G.B., Helland,A., Borresen-Dale,A.L. *et al.* (2006) Gene expression programs in response to hypoxia: cell type specificity and prognostic significance in human cancers. *PLoS Med.*, **3**, e47.

83. Jogi,A., Ora,I., Nilsson,H., Lindeheim,A., Makino,Y., Poellinger,L., Axelson,H. and Pahlman,S. (2002) Hypoxia alters gene expression in human neuroblastoma cells toward an immature and neural crest-like phenotype. *Proc. Natl. Acad. Sci. U.S.A.*, **99**, 7021–7026.

84. Bratasz,A., Pandian,R.P., Deng,Y., Petryakov,S., Grecula,J.C., Gupta,N. and Kuppusamy,P. (2007) In vivo imaging of changes in tumor oxygenation during growth and after treatment. *Magn. Reson. Med.*, **57**, 950–959.

85. Madan,E., Parker,T.M., Bauer,M.R., Dhiman,A., Pelham,C.J., Nagane,M., Kuppusamy,M.L., Holmes,M., Holmes,T.R., Shaik,K. *et al.* (2018) The curcumin analog HO-3867 selectively kills cancer cells by converting mutant p53 protein to transcriptionally active wildtype p53. *J. Biol. Chem.*, **293**, 4262–4276.

86. Xia,X.B., Lemieux,M.E., Li,W., Carroll,J.S., Brown,M., Liu,X.S. and Kung,A.L. (2009) Integrative analysis of HIF binding and transactivation reveals its role in maintaining histone methylation homeostasis. *Proc. Natl. Acad. Sci. U.S.A.*, **106**, 4260–4265.

87. Schindl,M., Bachtiary,B., Dreier,B., Birner,P., Latinovic,L., Karner,B., Breitenecker,G. and Oberhuber,G. (2001) Impact of human papillomavirus infection on the expression of the KAI1

metastasis suppressor protein in invasive cervical cancer. *Cancer Lett.*, **162**, 261–266.

88. Sharma,A.K., Ali,A., Gogna,R., Singh,A.K. and Pati,U. (2009) p53 Amino-terminus region (1-125) stabilizes and restores heat denatured p53 wild phenotype. *PLoS One*, **4**, e7159.

89. Madan,E., Pelham,C.J., Nagane,M., Parker,T.M., Canas-Marques,R., Fazio,K., Shaik,K., Yuan,Y., Henriques,V., Galzerano,A. *et al.* (2019) Flower isoforms promote competitive growth in cancer. *Nature*, **572**, 260–264.

90. Madan,E., Gogna,R., Kuppusamy,P., Bhatt,M., Pati,U. and Mahdi,A.A. (2012) TIGAR induces p53-mediated cell-cycle arrest by regulation of RB-E2F1 complex. *Br. J. Cancer*, **107**, 516–526.

91. Shieh,S.Y., Ikeda,M., Taya,Y. and Prives,C. (1997) DNA damage-induced phosphorylation of p53 alleviates inhibition by MDM2. *Cell*, **91**, 325–334.

92. Thomas,M.C. and Chiang,C.M. (2005) E6 oncoprotein represses p53-dependent gene activation via inhibition of protein acetylation independently of inducing p53 degradation. *Mol. Cell*, **17**, 251–264.

93. Gogna,R., Madan,E., Khan,M., Pati,U. and Kuppusamy,P. (2013) p53′s choice of myocardial death or survival: Oxygen protects infarct myocardium by recruiting p53 on NOS3 promoter through regulation of p53-Lys(118) acetylation. *EMBO Mol. Med.*, **5**, 1662–1683.

94. An,W.G., Kanekal,M., Simon,M.C., Maltepe,E., Blagosklonny,M.V. and Neckers,L.M. (1998) Stabilization of wild-type p53 by hypoxia-inducible factor 1alpha. *Nature*, **392**, 405–408.

95. Baugh,E.H., Ke,H., Levine,A.J., Bonneau,R.A. and Chan,C.S. (2018) Why are there hotspot mutations in the TP53 gene in human cancers? *Cell Death Differ.*, **25**, 154–160.

96. Cole,A.J., Zhu,Y., Dwight,T., Yu,B., Dickson,K.A., Gard,G.B., Maidens,J., Valmadre,S., Gill,A.J., Clifton-Bligh,R. *et al.* (2017) Comprehensive analyses of somatic TP53 mutation in tumors with variable mutant allele frequency. *Sci. Data*, **4**, 170120.

97. Wang,X. and Sun,Q. (2017) TP53 mutations, expression and interaction networks in human cancers. *Oncotarget*, **8**, 624–643.

98. Forsythe,J.A., Jiang,B.H., Iyer,N.V., Agani,F., Leung,S.W., Koos,R.D. and Semenza,G.L. (1996) Activation of vascular endothelial growth factor gene transcription by hypoxia-inducible factor 1. *Mol. Cell Biol.*, **16**, 4604–4613.

99. Cartharius,K., Frech,K., Grote,K., Klocke,B., Haltmeier,M., Klingenhoff,A., Frisch,M., Bayerlein,M. and Werner,T. (2005) MatInspector and beyond: promoter analysis based on transcription factor binding sites. *Bioinformatics*, **21**, 2933–2942.

100. Natan,E., Baloglu,C., Pagel,K., Freund,S.M., Morgner,N., Robinson,C.V., Fersht,A.R. and Joerger,A.C. (2011) Interaction of the p53 DNA-binding domain with its n-terminal extension modulates the stability of the p53 tetramer. *J. Mol. Biol.*, **409**, 358–368.

101. Ortiz-Barahona,A., Villar,D., Pescador,N., Amigo,J. and del Peso,L. (2010) Genome-wide identification of hypoxia-inducible factor binding sites and target genes by a probabilistic model integrating transcription-profiling data and in silico binding site prediction. *Nucleic Acids Res.*, **38**, 2332–2345.

102. Mole,D.R., Blancher,C., Copley,R.R., Pollard,P.J., Gleadle,J.M., Ragoussis,J. and Ratcliffe,P.J. (2009) Genome-wide Association of Hypoxia-inducible Factor (HIF)-1 alpha and HIF-2 alpha DNA binding with expression profiling of Hypoxia-inducible Transcripts. *J. Biol. Chem.*, **284**, 16767–16775.

103. Theodoropoulos,V.E., Lazaris,A.C., Kastriotis,I., Spiliadi,C., Theodoropoulos,G.E., Tsoukala,V., Patsouris,E. and Sofras,F. (2005) Evaluation of hypoxia-inducible factor 1 alpha overexpression as a predictor of tumour recurrence and progression in superficial urothelial bladder carcinoma. *BJU Int.*, **95**, 425–431.

104. Liu,L., Zhang,P., Bai,M., He,L., Zhang,L., Liu,T., Yang,Z., Duan,M., Liu,M., Liu,B. *et al.* (2018) p53 upregulated by HIF-1alpha promotes hypoxia-induced G2/M arrest and renal fibrosis in vitro and in vivo. *J. Mol. Cell Biol.*, **11**, 371–382.

105. Zhou,C.H., Zhang,X.P., Liu,F. and Wang,W. (2015) Modeling the interplay between the HIF-1 and p53 pathways in hypoxia. *Sci. Rep.*, **5**, 13834.

106. Chen,B.S., Longtine,M.S., Sadovsky,Y. and Nelson,D.M. (2010) Hypoxia downregulates p53 but induces apoptosis and enhances expression of BAD in cultures of human syncytiotrophoblasts. *Am. J. Physiol.-Cell Ph*, **299**, C968–C976.

107. Ashcroft,M., Taya,Y. and Vousden,K.H. (2000) Stress signals utilize multiple pathways to stabilize p53. *Mol. Cell Biol.*, **20**, 3224–3233.

108. Suzuki,H., Tomida,A. and Tsuruo,T. (2001) Dephosphorylated hypoxia-inducible factor 1 alpha as a mediator of p53-dependent apoptosis during hypoxia. *Oncogene*, **20**, 5779–5788.

109. Anderson,C.W. and Appella,E. (2010) In: Bradshaw,R.A. and Dennis,E.A. (eds). *Handbook of Cell Signaling (Second Edition)*. Academic Press, San Diego, pp. 2185–2204.

110. Cooks,T., Pateras,I.S., Tarcic,O., Solomon,H., Schetter,A.J., Wilder,S., Lozano,G., Pikarsky,E., Forshew,T., Rosenfeld,N. *et al.* (2013) Mutant p53 Prolongs NF-kappa B activation and promotes chronic inflammation and Inflammation-associated colorectal cancer. *Cancer Cell*, **24**, 272–272.

111. Dong,P., Karaayvaz,M., Jia,N., Kaneuchi,M., Hamada,J., Watari,H., Sudo,S., Ju,J. and Sakuragi,N. (2013) Mutant p53 gain-of-function induces epithelial-mesenchymal transition through modulation of the miR-130b-ZEB1 axis. *Oncogene*, **32**, 3286–3295.

112. Staller,P., Sulitkova,J., Lisztwan,J., Moch,H., Oakeley,E.J. and Krek,W. (2003) Chemokine receptor CXCR4 downregulated by von Hippel-Lindau tumour suppressor pVHL. *Nature*, **425**, 307–311.

113. Maxwell,P.H., Wiesener,M.S., Chang,G.W., Clifford,S.C., Vaux,E.C., Cockman,M.E., Wykoff,C.C., Pugh,C.W., Maher,E.R. and Ratcliffe,P.J. (1999) The tumour suppressor protein VHL targets hypoxia-inducible factors for oxygen-dependent proteolysis. *Nature*, **399**, 271–275.

114. Iliopoulos,O., Ohh,M. and Kaelin,W.G. Jr. (1998) pVHL19 is a biologically active product of the von Hippel-Lindau gene arising from internal translation initiation. *Proc. Natl. Acad. Sci. U.S.A.*, **95**, 11661–11666.

115. Schito,L., Rey,S., Tafani,M., Zhang,H., Wong,C.C., Russo,A., Russo,M.A. and Semenza,G.L. (2012) Hypoxia-inducible factor 1-dependent expression of platelet-derived growth factor B promotes lymphatic metastasis of hypoxic breast cancer cells. *Proc. Natl. Acad. Sci. U.S.A.*, **109**, E2707–E2716.

116. Kotch,L.E., Iyer,N.V., Laughner,E. and Semenza,G.L. (1999) Defective vascularization of HIF-1alpha-null embryos is not associated with VEGF deficiency but with mesenchymal cell death. *Dev. Biol.*, **209**, 254–267.

117. Yu,A.Y., Shimoda,L.A., Iyer,N.V., Huso,D.L., Sun,X., McWilliams,R., Beaty,T., Sham,J.S., Wiener,C.M., Sylvester,J.T. *et al.* (1999) Impaired physiological responses to chronic hypoxia in mice partially deficient for hypoxia-inducible factor 1alpha. *J. Clin. Invest.*, **103**, 691–696.

118. Wang,Y., Wan,C., Deng,L., Liu,X., Cao,X., Gilbert,S.R., Bouxsein,M.L., Faugere,M.C., Guldberg,R.E., Gerstenfeld,L.C. *et al.* (2007) The hypoxia-inducible factor alpha pathway couples angiogenesis to osteogenesis during skeletal development. *J. Clin. Invest.*, **117**, 1616–1626.

119. Zehetner,J., Danzer,C., Collins,S., Eckhardt,K., Gerber,P.A., Ballschmieter,P., Galvanovskis,J., Shimomura,K., Ashcroft,F.M., Thorens,B. *et al.* (2008) PVHL is a regulator of glucose metabolism and insulin secretion in pancreatic beta cells. *Genes Dev.*, **22**, 3135–3146.

120. Cramer,T., Yamanishi,Y., Clausen,B.E., Forster,I., Pawlinski,R., Mackman,N., Haase,V.H., Jaenisch,R., Corr,M., Nizet,V. *et al.* (2003) HIF-1alpha is essential for myeloid cell-mediated inflammation. *Cell*, **112**, 645–657.

121. Bohuslavova,R., Cerychova,R., Papousek,F., Olejnickova,V., Bartos,M., Görlach,A., Kolar,F., Sedmera,D., Semenza,G.L. and Pavlinkova,G. (2019) HIF-1α is required for development of the sympathetic nervous system. *Proc. Natl. Acad. Sci. U.S.A.*, **116**, 13414–13423.

122. Sano,M., Minamino,T., Toko,H., Miyauchi,H., Orimo,M., Qin,Y., Akazawa,H., Tateno,K., Kayama,Y., Harada,M. *et al.* (2007) p53-induced inhibition of Hif-1 causes cardiac dysfunction during pressure overload. *Nature*, **446**, 444–448.